การศึกษาเชิงเปรียบเทียบและการปรับปรุงความเร็วการถ่ายภาพด้วยรังสีโดยใช้ฟิล์มสำหรับการตรวจสอบชิ้นงานอุตสาหกรรมโดยไม่ทำลาย

นายเฉลิมพงษ์ โพธิ์ลี้

วิทยานิพนธ์นี้เป็นส่วนหนึ่งของการศึกษาตามหลักสูตรปริญญาวิศวกรรมศาสตรดุษฎีบัณฑิต
สาขาวิชาวิศวกรรมนิวเคลียร์ ภาควิชาวิศวกรรมนิวเคลียร์
คณะวิศวกรรมศาสตร์ จุฬาลงกรณ์มหาวิทยาลัย
ปีการศึกษา 2558

Comparative Investigation and Improvement of Film Radiography Speed for Non-Destructive Inspection of Industrial Specimens

Mr. Chalermpong Polee

A Dissertation Submitted in Partial Fulfillment of the Requirements
for the Degree of Doctor of Engineering Program in Nuclear Engineering
Department of Nuclear Engineering
Faculty of Engineering
Chulalongkorn University
Academic Year 2015

Thesis Title	Comparative Investigation and Improvement of Film Radiography Speed for Non-Destructive Inspection of Industrial Specimens
By	Mr. Chalermpong Polee
Field of Study	Nuclear Engineering
Thesis Advisor	Associate Professor Nares Chankow
Thesis Co-Advisor	Associate Professor Somyot Srisatit

Accepted by the Faculty of Engineering, Chulalongkorn University in Partial Fulfillment of the Requirements for the Doctoral Degree

....Dean of the Faculty of Engineering
(Professor Bundhit Eua-arporn, Ph.D.)

THESIS COMMITTEE

....Chairman
(Associate Professor Sunchai Nilsuwankosit, Ph.D.)

....Thesis Advisor
(Associate Professor Nares Chankow)

....Thesis Co-Advisor
(Associate Professor Somyot Srisatit)

....Examiner
(Somboon Rassame, Ph.D.)

....Examiner
(Phongphaeth Pengvanich, Ph.D.)

....External Examiner
(Associate Professor Raewat Laopaiboon)

เฉลิมพงษ์ โพธิ์ลี้ : การศึกษาเชิงเปรียบเทียบและการปรับปรุงความเร็วการถ่ายภาพด้วยรังสีโดยใช้ฟิล์มสำหรับการตรวจสอบชิ้นงานอุตสาหกรรมโดยไม่ทำลาย (Comparative Investigation and Improvement of Film Radiography Speed for Non-Destructive Inspection of Industrial Specimens) อ.ที่ปรึกษาวิทยานิพนธ์หลัก: รศ. นเรศร์ จันทน์ขาว, อ.ที่ปรึกษาวิทยานิพนธ์ร่วม: รศ. สมยศ ศรีสถิตย์, 95 หน้า.

การถ่ายภาพด้วยรังสีโดยใช้ฟิล์มบันทึกภาพยังคงถูกใช้งานอย่างกว้างขวางในงานอุตสาหกรรม ถึงแม้ว่าประสิทธิภาพในการบันทึกภาพของฟิล์มน้อยกว่า 1% และต่ำกว่ามากในช่วงพลังงานสูงขึ้น แผ่นบันทึกภาพมีความเร็วสูงกว่าฟิล์มมากกว่า 10 เท่า แต่เครื่องอ่านข้อมูลภาพและแผ่นบันทึกภาพมีราคาสูง รวมทั้งยังมีปัญหาเกี่ยวกับการเลือนหายของข้อมูลภาพ งานวิจัยนี้มุ่งศึกษา พัฒนาเทคนิคการเพิ่มความเร็วโดยการใช้ฉากเพิ่มความเข้มของภาพชนิด PI-200 ซึ่งเป็นแกโดลิเนียมออกซีซัลไฟด์ จากการใช้ฉากชนิด PI-200 พบว่าค่าอินเทนซิฟายอิงแฟกเตอร์มีค่าประมาณ 33.6, 39.0 และ 61.3 สำหรับรังสีเอกซ์ที่ 100, 130 และ 160 kVp ในขณะที่วิธีปัจจุบันที่ใช้ฉากตะกั่วมีค่าอินเทนซิฟายอิงแฟกเตอร์ประมาณ 2.8, 3.4 และ 4.0 ตามลำดับ สำหรับรังสีแกมมาจากต้นกำเนิดรังสีอิริเดียม-192 และโคบอลต์-60 พบว่าฉาก PI-200 ให้ค่าอินเทนซิฟายอิงแฟกเตอร์ประมาณ 13.7 และ 7.3 ตามลำดับ ในขณะที่วิธีปัจจุบันที่ใช้ฉากตะกั่วมีค่าอินเทนซิฟายอิงแฟกเตอร์ประมาณ 5.8 และ 1.4 ตามลำดับ ซึ่งสรุปได้ว่าฉาก PI-200 สามารถเพิ่มความเร็วในการถ่ายภาพได้อย่างน้อย 2 เท่า โดยขึ้นอยู่กับพลังงานของรังสี นอกจากนั้นยังพบว่าความไวมีค่าเทียบเคียงกับการใช้ฉากตะกั่วแบบเดิม จากการใช้แผ่นกรองรังสีที่ทำจากตะกั่วพบว่าคุณภาพของภาพดีขึ้นเนื่องจากการตัดรังสีกระเจิงบางส่วนออกไป โดยเฉพาะอย่างยิ่งเมื่อชิ้นงานมีธาตุเบาเป็นองค์ประกอบ เช่น คอนกรีต นอกจากนี้งานวิจัยยังมีวัตถุประสงค์ในการพัฒนาอุปกรณ์สำหรับหาเวลาในการถ่ายภาพโดยไม่ต้องทราบข้อมูลเกี่ยวกับชนิดของธาตุและความหนาของตัวอย่าง ความแรงรังสีของต้นกำเนิด และระยะห่างจากต้นกำเนิดรังสีถึงฟิล์ม อุปกรณ์นี้อาศัยหลักการวัดความเข้มของรังสีเอกซ์หรือรังสีแกมมาที่ทะลุผ่านชิ้นงานด้วย PIN โฟโตไดโอดขนาดเล็ก หัววัดรังสีชนิดนี้ติดตั้งอยู่กับหน่วยจัดการสัญญาณพัลส์ และไมโครคอนโทรลเลอร์บอร์ด ซึ่งเชื่อมต่อกับโมดูลบลูทูธ ข้อมูลจำนวนนับรังสีถูกส่งไปแสดงผลบนจอสมาร์ทโฟนทันที โดยได้ออกแบบให้แอพพลิเคชันซอฟต์แวร์สามารถควบคุมและแสดงผลการนับรังสีได้ ก่อนการถ่ายภาพด้วยฟิล์มจะใช้อุปกรณ์นี้วางไว้ด้านหลังชิ้นงานในตำแหน่งที่ต้องการเพื่อวัดความเข้มรังสีทะลุผ่าน ซึ่งแปรผกผันกับเวลาในการถ่ายภาพด้วยรังสี ซึ่งสามารถทราบเวลาถ่ายภาพได้โดยไม่ต้องทราบข้อมูลเกี่ยวกับชนิดของธาตุและความหนาของตัวอย่าง ความแรงรังสีของต้นกำเนิด และระยะห่างจากต้นกำเนิดรังสีถึงฟิล์ม อย่างเช่นวิธีที่ใช้กันอยู่ในปัจจุบัน ในขั้นสุดท้ายได้ทำการทดลองถ่ายภาพชิ้นงาน 3 ชิ้น ที่มีความหนาต่างกันเพื่อให้มีความดำ 2.0 ตรงบริเวณที่กำหนด ผลการทดสอบพบว่า ได้ความดำมีค่าเท่ากับ 1.92, 1.98 และ 2.05 ซึ่งถือว่าใกล้เคียงกับค่าความดำที่ต้องการอย่างน่าพอใจ ซึ่งสามารถสรุปได้ว่าเทคนิคและอุปกรณ์ที่พัฒนาขึ้นสามารถทำให้กระบวนการถ่ายภาพด้วยรังสีประหยัด สะดวก และมีความเชื่อมั่นสูงขึ้น

ภาควิชา วิศวกรรมนิวเคลียร์	ลายมือชื่อนิสิต ....
สาขาวิชา วิศวกรรมนิวเคลียร์	ลายมือชื่อ อ.ที่ปรึกษาหลัก ....
ปีการศึกษา 2558	ลายมือชื่อ อ.ที่ปรึกษาร่วม ....

5471404321 : MAJOR NUCLEAR ENGINEERING

KEYWORDS: INTENSIFYING SCREEN / EXPOSURE TIME / INDUSTRIAL RADIOGRAPHY

CHALERMPONG POLEE: Comparative Investigation and Improvement of Film Radiography Speed for Non-Destructive Inspection of Industrial Specimens. ADVISOR: ASSOC. PROF. NARES CHANKOW, CO-ADVISOR: ASSOC. PROF. SOMYOT SRISATIT, 95 pp.

Film radiography is still used extensively in industry even though the image recording efficiency of the film is lower than <1% and is much lower at high energy range. The imaging plate is >10 times more sensitive than the conventional screen-film technique but its image reader and the imaging plate are relatively costly. Fading of the image data on the IP is also a problem. This research first emphasizes on improvement of the screen/film speed to reduce the exposure time by using the new PI-200 gadolinium oxysulfide (GOS) fluorescent screen. By using the PI-200 screens, the intensifying factors were found to be approximately 33.6, 39.0 and 61.3 for 100, 130 and 160 kVp x-rays while the IF's of the conventional lead screens were approximately 2.8, 3.4 and 4.0 respectively. The intensifying factors (IF) for ^{192}Ir and ^{60}Co gamma-rays were found to be approximately 13.7 and 7.3 respectively while the IF's of the conventional lead screens were approximately 5.8 and 1.4 respectively. The PI-200 screen thus could increase the speed of the conventional lead screen-film by at least 2 times depending on photon energy. Moreover, the sensitivity of the radiographs obtained from the PI-200 was comparable to those obtained from the conventional lead screen film technique. It was also found that the image quality could significantly improve by using lead filter to absorb the scattered gamma-rays at low energy range particularly when the specimens contained light elements such as concrete. In addition, objective of this research was to develop a device to determine the exposure time without need of information on the test specimen such as kind of material and thickness, source activity and source-to-film distance. The device was based on measurement of the transmitted x-ray or gamma-ray intensity by using a small PIN photodiode detector. The detector was mounted with a pulse processing unit and a microcontroller board and connected to a Bluetooth module. The counting data could simultaneously send to a smartphone to display the intensity. Application software was developed to control the measurement as well as to display the counting data. Prior to film exposure, the device was placed behind the specimen at required position to measure transmitted intensity which was inversely proportional to the exposure. Unlike in using the conventional exposure curve, correction factors for source decay, source-to-film distance, specimen thickness and kind of material were not needed. The developed technique and device was finally tested in radiography of the three specimens having different thicknesses to obtain a film density of 2.0 on the required areas. The obtained film densities on the required areas were found to be 1.92, 1.98 and 2.05 which were very satisfactory. The developed technique and device could the make radiographic process economic, convenient and more reliable.

Department:	Nuclear Engineering	Student's Signature	....
Field of Study:	Nuclear Engineering	Advisor's Signature	....
Academic Year:	2015	Co-Advisor's Signature	....

ACKNOWLEDGEMENTS

The success of my dissertation would not have been possible without the support from many people. I would like to distribute my gratitude to all those people.

Foremost, I would greatly appreciate my advisor, Assoc. Prof. Nares Chankow who provided me guidance, advices, and kind helps. He attentively gave me comments and corrections for my drafts of doctoral thesis. I owe you a lot. Moreover, I deeply appreciate my co-advisor and committee members for this dissertation, Assoc. Prof. Somyot Srisatit, Assoc. Prof. Raewat Laopaiboon, Dr. Somboon Rassame and Dr. Phongphaeth Pengvanich for their comments, and discussion on this work.

My gratitude is extended to Non-destructive Testing Divison of Nuclear Service Center, Thailand Institute of Technology (Public organization) for supporting the radiographic facility with Co-60 radiation source and Thai Non-destructive Testing Public Company Limited, for providing me Ir-192 projector.

Many thanks are distributed to all of professors, administration staffs of Nuclear Engineering department and my colleagues who provided me the kind support.

At last, I would like to express the greatest gratitude to my family for their sincere support, authentic encouragement and immeasurably love.

CONTENTS

Page

Page

Page

List of Table

List of Figure

CHAPTER 1
INTRODUCTION

1.1 Background and problems of interest

Non-Destructive Testing (NDT) has played vital roles in industry, research and development worldwide. Common NDT methods include visual testing (VT), liquid penetrant testing (PT), magnetic particle testing (MT), ultrasonic testing (UT), Eddy Current Testing (ET) and radiographic testing (RT). UT and RT are used widely in industry than other methods due to their capabilities in detecting minute defects hidden inside the specimens. Radiographic testing using x-ray and gamma ray is one of the nondestructive testing methods widely used for inspection of industrial specimens including raw materials and finished products as well as for routine inspection of parts during operation. The advantage of radiography is fast inspection of wide variety of material types with varying density. Moreover, radiography can inspect assembled components, finished products or parts of engines, automobiles and aircrafts to look for defects, foreign materials, misalignment and corrosion areas. RT has advantages for providing permanent record and interpretation can be easily understood by most people.

X-ray generator and radioisotopic gamma ray source are employed to produce x-rays and gamma rays in industrial radiography respectively. The choice of radioactive source and strength depend on many factors including material type, thickness, and density. The different transmitted gamma ray after pass through a specimen will interact with an image recorder to provide image. Film has been used as a recording medium but it is gradually replaced by imaging plate (IP), linear detector and flat panel detector. However, film is still mainly used for industrial RT. One problem of film radiography is having very low recording efficiency i.e. less than 1% except for energy below 100 keV. The efficiency is even much lower at higher energy range. This makes high energy film radiography impractical. Therefore the film is practically placed in between two intensifying screens to reduce the exposure time by converting part of x-rays or gamma rays to electrons or light photons [1-4]. Film blackening is thus caused by direct interaction of x-ray or gamma-ray photons with film and indirect interaction with the screens. There are three types of intensifying screens i.e. lead foil screen, fluorescent screen and fluorometallic screen. Lead foil screens composing of lead (Pb) and antimony (Sb) are commonly used in industrial RT above 100 keV. Film is placed in between two lead screens during exposure. The screens convert x-ray and gamma ray photons to electrons causing film blackening resulting in reduction of the exposure time. Unfortunately, the conversion efficiency of the lead foil screen decreases with increasing of photon energy. The fluorescent screen consists of phosphor material which emits light photons from interaction with radiation. Recently, manufacturers have developed fluorescent screens which give better response to high energy radiation gamma-rays in MeV range such as PI200 screen manufactured by Mitsubishi Chemical Corporation. Increase in conversion efficiency of the intensifying screen and recording efficiency of the film are the key factors in improving speed of the RT techniques. For thick specimens containing light elements such as concrete structure, scattered x-rays or gamma rays can cause unsharpness and low contrast image. Removal of scattered radiation can improve the image quality.

This research aimed to improve speed of industrial x-ray and gamma-ray radiographic techniques using film and to develop a device for determining the exposure time without knowledge of specimen thickness, hollowness, kind of material, source activity and specimen-to-film distance. The developed technique and exposure device will make the industrial radiography process faster, more reliable and economical. Investigation of properties of the available intensifying screens such as intensifying factor, resolution and compatibility was first carried out.

1.2 Dissertation objective

1.2.1 To investigate industrial x-ray and gamma-ray radiographic techniques commonly used for nondestructive testing (NDT) of materials and to identify weaknesses that cause limitations of the film radiographic techniques.

1.2.2 To improve speed of industrial x-ray and gamma-ray radiographic techniques using film taking into account image quality as well as economical and practical aspects.

1.2.3 To develop a new method for determining the exposure time which is independent on specimen thickness, material type, source activity and source-to-film distance.

1.3 Scope of dissertation

1.3.1 Investigate factors affecting the specimen image qualities from radiographic techniques using film such as sharpness, contrast and resolution for gamma ray sources and x-ray generators.

1.3.2 Investigate properties for each intensifying screen, such as emission wavelength, efficiency and sensitivity, to match with each film type.

1.3.3 Develop technique for improving radiography speed based on the investigated results.

1.3.4 Apply and evaluate the image quality obtained from the developed technique in comparison to those obtained from the conventional technique.

1.3.5 Design and construct the alternative new method to determine the exposure time for gamma ray radiography by using small detector counting system.

1.3.6 Test and evaluate the developed device and technique in determining the exposure time for some industrial test specimens.

1.4 Expected benefit

1.4.1 The radiographic technique and components developed from this research can be used for routine inspection of specimens with improvement in speed and image quality.

1.4.2 The developed device and method can give radiographers the required exposure to obtain the desired film density without knowledge of specimen material, specimen thickness, source distance and the remaining source strength.

1.5 Research methodology

1.5.1 Review literature.

1.5.2 Investigate factors affecting the specimen image qualities from radiographic techniques using film, such as sharpness, contrast and resolution for gamma sources and x-ray generators.

1.5.3 Investigate properties for each intensifying screen, such as emission wavelength, efficiency and sensitivity, to match with screen convertor for each film type.

1.5.4 Develop technique for improving radiography speed based on the investigated results.

1.5.5 Apply and evaluate the image quality obtained from the developed technique in comparison to those obtained from the conventional technique.

1.5.6 Design and construct the alternative new method to determine the exposure time for gamma ray radiography by using small detector counting system.

1.5.7 Test and evaluate the developed device and technique in determining the exposure time for some industrial test specimens.

1.5.8 Analyze result and discussion.

1.5.9 Conclusion

CHAPTER 2
THEORY AND LETERATURE REVIEW

2.1 Principle of radiography technique (RT)

In radiographic testing, the part to be inspected is placed between the radiation source and a piece of radiation sensitive film, as shown in figure 2.1. The radiation source can either be an x-ray machine or a radioactive source. The part will stop some of the radiation where thicker and more dense area. The radiation that passes through the part will expose the film and forms a shadowgraph of the part. The film darkness density of film is varied with the amount of radiation reaching the film through the test object where darker areas indicate more exposure (higher radiation intensity) and liter areas indicate less exposure (lower radiation intensity). This variation in the image darkness can be used to determine thickness or composition of material and to reveal the presence of any flaws or discontinuities inside material.

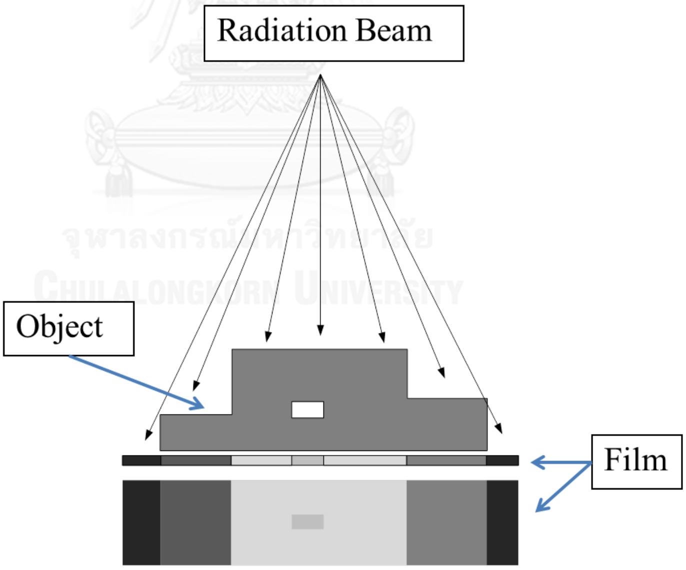

Figure 2.1 Principle of radiography technique

The reduction in radiation intensity on penetrating a material is determined by the following interactions:

- Photoelectric effect
- Compton effect
- Pair production

Which of these interactions will predominate depends on the energy of the incident radiation and the material atomic number.

2.1.1 Photoelectric effect

When x-rays or gamma ray pass through a material and a photon collides with an atom of this material, the total energy of this photon can be used to eject an electron from the inner shells of the atom, as Figure 2.2 illustrates. This phenomenon is called the photoelectric effect and occurs in the object, in the film and in any filters used.

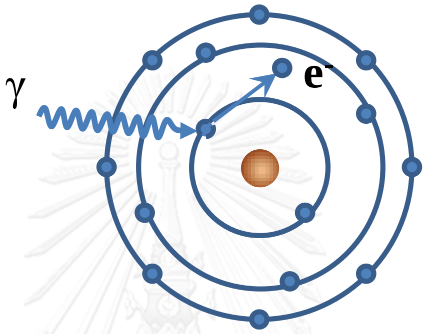

Figure 2.2 Photoelectric effect reaction

2.1.2 Compton effect

With higher x-ray energies (100 keV to 10 MeV), the interaction of photons with free or weakly bonded electrons of the outer atom layers causes part of the energy to be transferred to these electrons which are then ejected, as illustrated figure 2.3. At the same time the photons will be deflected from the initial angle of incidence and emerge from the collision as radiation of reduced energy, scattered in all directions including backward, known as “back-scatter”, In this energy band, the absorption of radiation is mainly due to the Compton effect and less so to the photoelectric effect

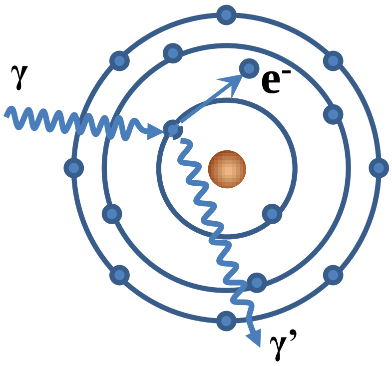

Figure 2.3 Compton effect

2.1.3 Pair production

The formation of ion pairs, see figure 2.4, only occurs at very high energy levels (above 1.022 MeV). High-energy photons can cause an interaction with the nucleus of the atom involved in the collision. The energy of the photon is here used to eject an electron (e^-) and a positron (e^+)

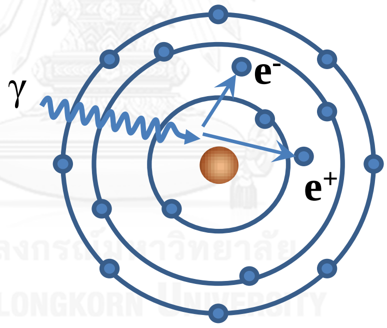

Figure 2.4 Pair production reaction

The intensity of a beam of x-rays or gamma rays suffers a loss of intensity while passing through a material. This phenomenon is due to the absorption or scattering of the x-ray or gamma rays by the object being exposed. The amount of radiation lost depends on the quality of radiation, the density of the material and the thickness traversed. The beam of radiation, which emerges from the material, is usually used to expose a radiation sensitive film so that different intensities of radiation are displayed as different densities on the film.

The relationship between intensity of the incident and the transmitted photons follows Lambert's law as in equation (2.1).

$$I = I_0 e^{-\mu x} \tag{2.1}$$

where

I is the transmitted photon intensity unit is $cm^2 .s^{-1}$,

I_0 is the incident photon intensity unit is $cm^2 .s^{-1}$,

μ is the attenuation coefficient unit is cm^{-1},

X is thickness of the specimen unit is cm.

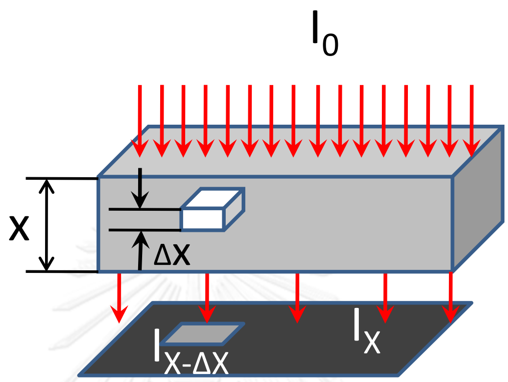

Figure 2.5 shown the image of defect on film which agree with position of defect and the direction of beam

From figure 2.5, $I_{X-\Delta X}$ is intensity of photon that penetrated the defect as ΔX and is equation to $I_{X-\Delta X} = I_0 e^{-\mu(X-\Delta X)}$

so $$\frac{I_{X-\Delta X}}{I_X} = \frac{e^{[-\mu(X-\Delta X)]}}{e^{[-\mu X]}} = e^{[\mu \Delta X]}$$

(2.2)

$$\ln\left[\frac{I_{X-\Delta X}}{I_X}\right] = \mu \Delta X \tag{2.3}$$

$$2.303(\log I_{X-\Delta X} - \log I_X) = \mu \Delta X \tag{2.4}$$

$$\log I_{X-\Delta X} - \log I_X = 0.434\, \mu \Delta X \tag{2.5}$$

where

G_D is film gradient or slope between film density and relative exposure logarithm

$$G_D\,[\log I_{X-\Delta X} - \log I_X] = 0.434\, \mu \Delta X G_D$$

$$D_{X-\Delta X} - D_X = 0.434\ \mu\Delta X G_D$$
$$\Delta D = 0.434\ \mu\Delta X G_D \tag{2.6}$$

Then ΔD is different of film density between defect and non-defect of specimen

2.2 Film [5]

X-ray film for general radiography consist of emulsion-gelatin containing radiation sensitive silver halide crystals, such as silver bromide or silver chloride, and a flexible, transparent, blue-tinted base. The emulsion is different from those used in other types of photography films to account for the distinct characteristics of gamma rays and x-rays, but x-ray films are sensitive to light. Usually, the emulsion is coated on both sides of the base in layers about 0.0005 inches thick. Putting emulsion on both sides of the base doubles the amount of radiation-sensitive silver halide, and thus increases the film speed, as shown in figure 2.6

When x-rays, gamma rays, or light strike the grains of the sensitive silver halide in the emulsion, some of the Br^- ions are liberated and captured by the Ag^+ ions. This change is of such a small nature that it cannot be detected by ordinary physical methods and is called a "latent (hidden) image." However, the exposed grains are now more sensitive to the reduction process when exposed to a chemical solution (developer), and the reaction results in the formation of black, metallic silver. It is this silver, suspended in the gelatin on both sides of the base, which creates an image.

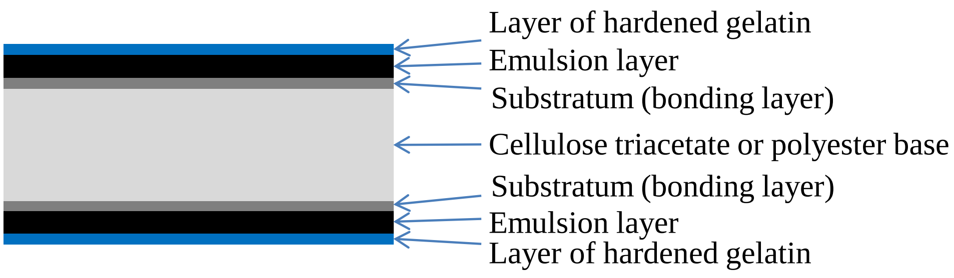

Figure 2.6 Schematic cross-section of x-ray film

2.3 Intensifying screen

The radiographic image is formed by only approximately 1 % of the amount of radiation energy exposed at the film. The rest passes through the film and is consequently not used. To utilize more of the available radiation intensity, the film is sandwiched between two intensifying screens. Different types of material are being used for this purpose

2.3.1 Lead screen

Under the impact of x-rays and gamma rays, lead screens emit electrons to which the film is sensitive. In industrial radiography this effect is made use of: the film is placed between two layers of lead to achieve the intensifying effect and intensity improvement of approximately factor 4 can be realized. This method of intensification is used within the energy range of 80 keV to 420 keV, and applies equally to x-ray or gamma-radiation, such as produced by Iridium192. Intensifying screens are made up of two homogeneous sheets of lead foil (stuck on to a thin base such as a sheet of paper or cardboard) between which the film is placed: the so called front and back screens.

The thickness of the front screen (source side) must match the hardness of the radiation being used, so that it will pass the primary radiation while stopping as much as possible of the secondary radiation (which has a longer wavelength and is consequently less penetrating).

The lead foil of the front screen is usually 0.02 to 0.15 mm thick. The front screen acts not only as an intensifier of the primary radiation, but also as an absorbing filter of the softer scatter, which enters in part at an oblique angle. The thickness of the back screen is not critical and is usually approximately 0.25 mm.

The surface of lead screen is polished to allow as close a contact as possible with the surface of the film. Flaws such as scratches or cracks on the surface of the metal will be visible in the radiograph and must be avoided. There are also x-ray film cassettes on the market with built-in lead-screens and vacuum packed to ensure perfect contact between emulsion and lead foil surface

2.3.2 Fluorescent screen

The term fluorescence (often mistaken for phosphorescence) is used to indicate the characteristic of a substance to instantly emit light when interact with electromagnetic radiation. The moment radiation stops, so does the lighting effect as shown in figure 2.7. This phenomenon is made good use of in film based radiography. Certain substances emit so much light when subjected to ionizing radiation, that they have considerably more effect on the light sensitive film than the direct ionizing radiation itself. The figure 2.8 and 2.9 showed the optical emission spectra of each type of fluorescent screen compared with spectra sensitivity of standard silver halide x-ray film.

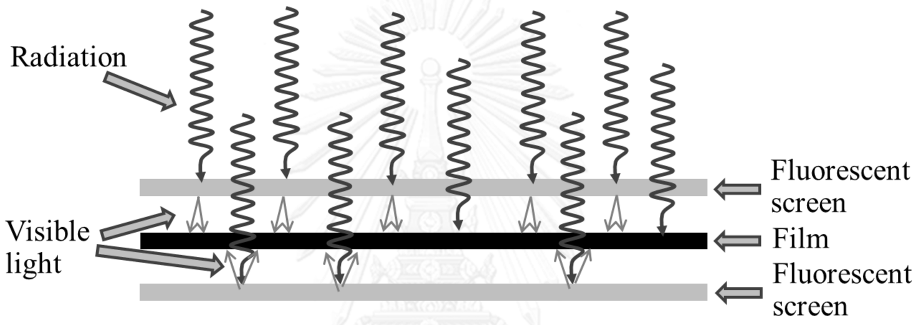

Figure 2.7 Illustration of light emission of fluorescent screen

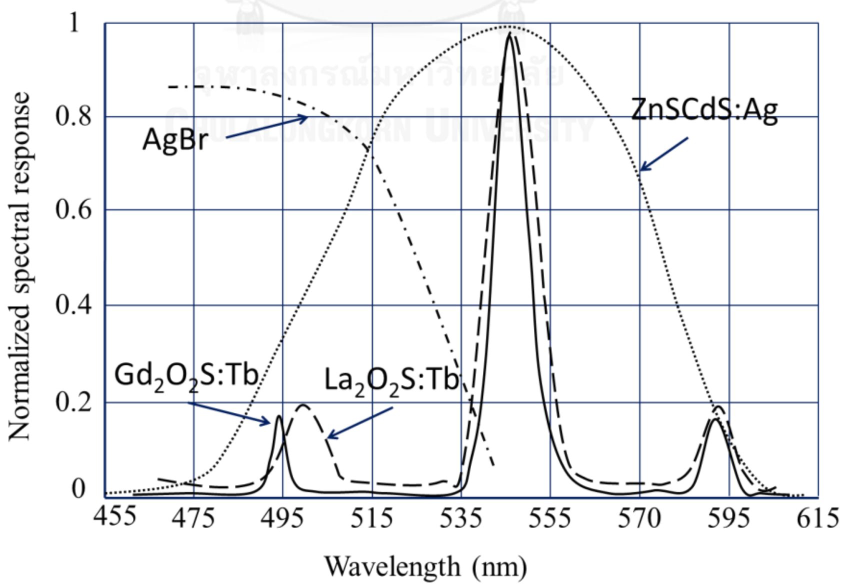

Figure 2.8 Optical emission spectra of Gd_20_2S:Tb, La_20_2S:Tb. Y_2O_2S:Tb and ZnSCdS:Ag scintillating screens compared with spectra sensitivity of standard silver halide x-ray film.[3]

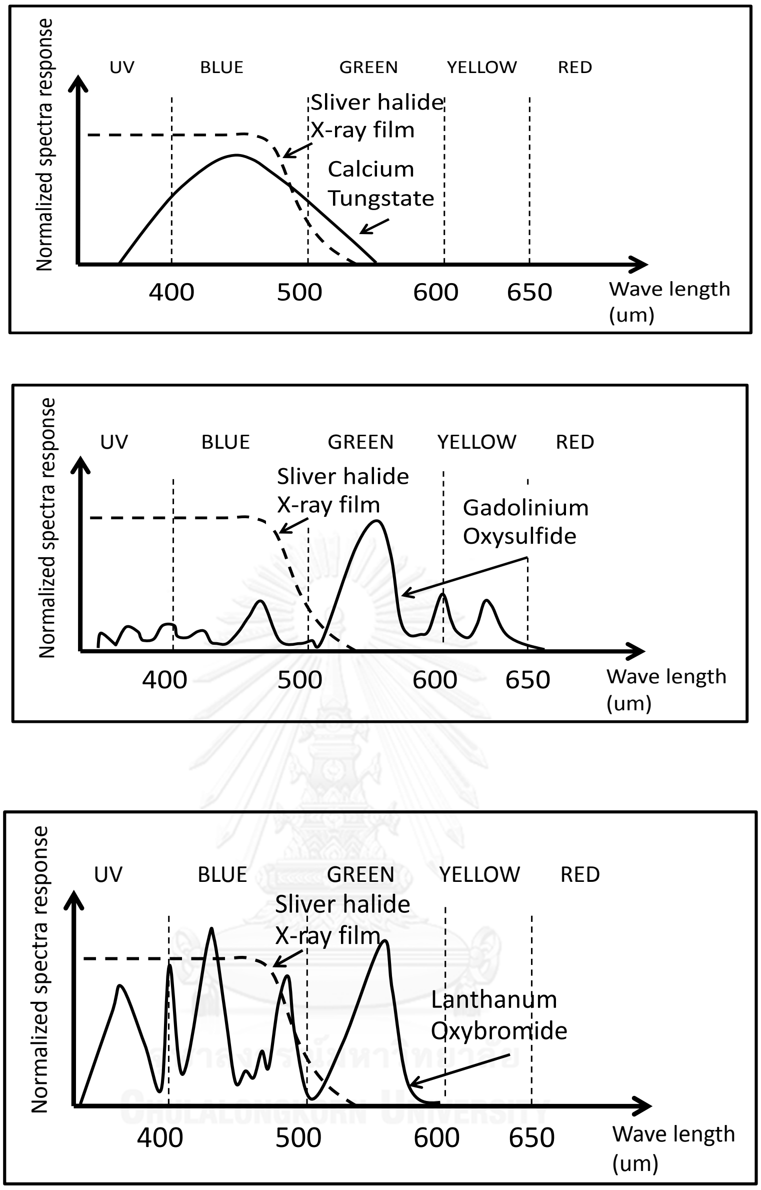

Figure 2.9 Spectral emissions of three phosphors as compared with the spectral sensitivity of standard silver halide x-ray film. This demonstrates how it is possible for some phosphors to be limited to use with only one film type while others can be used with both film types. [6]

2.3.3 Fluorometallic screen

Fluorometallic screens combine the advantages of both fluorescent and lead screen. It consists of a $CaWO_4$ layer combined with a lead layer and will permit useful reductions in exposure depending upon energy and exposure duration. Image definition is far better than with ordinary fluorescent screens, and the higher contrast produced by the light image emitted helps improve sensitivity of flaw detection.

2.4 Radioisotope source [7]

Manmade radioactive sources are produced by introducing an extra neutron to atoms of the source material. As the material gets rid of the neutron, energy is released in the form of gamma rays. Two of the most common industrial gamma ray sources for industrial radiography are Iridium-192 and Cobalt-60. In comparison to an x-ray generator, Iridium-192 to a 460 kV x-ray system and Cobalt-60 produces energies comparable to a 1.25 MV x-ray system as show in figure 2.12 and table 2.1.. These high energies make it possible to penetrate thick material with a relatively short exposure time. This and the fact that sources are very portable are the main reason that gamma sources are widely used for field radiography. Of course, the disadvantage of a radioactive source is that it can never be turned off and safely managing the source is a constant responsibility.

Physical size of isotope materials varies between manufacturers, but generally an isotope material is a pellet that measures 1.5 mm × 1.5 mm. Depending on the level of activity desired, a pellet or pellets are loaded into a stainless steel capsule and sealed by welding. The capsule is attached to short flexible cable called a pigtail, as shown in figure 2.10

Figure 2.10Source capsule and pigtail [7]

The source capsule and the pigtail are housed in a shielding device referred to as a exposure device or camera. Depleted uranium is often used as a shielding material for sources. The exposure device for Iridium-192 and Cobalt-60 sources will contain 22 kg and 225 kg of shielding materials, respectively as shown in figure 2.11. Cobalt cameras are often fixed to a trailer and transported to and from inspection sites. When the source is not being used to make an exposure, it is locked inside the exposure device. To make a radiographic exposure, a crank-out mechanism and a guide tube are attached to opposite ends of the exposure device. The guide tube often has a collimator (usually made of tungsten) at the end to shield the radiation except in the direction necessary to make the exposure. The end of the guide tube is secured in the location where the radiation source needs to be to produce the radiograph. The crank-out cable is stretched as far as possible to put as much distance as possible between the exposure device and the radiographer. To make the exposure, the radiographer quickly cranks the source out of the exposure device and into position in the collimator at the end of the guide tube. At the end of the exposure time, the source is cranked back into the exposure device. There is a series of safety procedures, which include several radiation surveys, which must be accomplished when making an exposure with a gamma source.

Figure 2.11 Shielding of radioactive source for Ir-192 (a), for Co-60 (b)

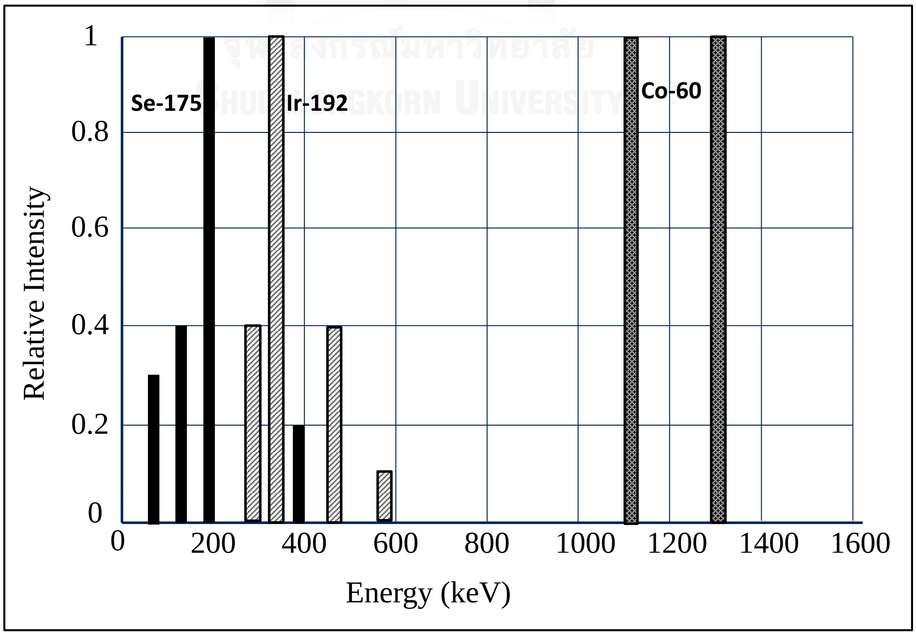

Figure 2.12 Spectrum radioactive source of Selenium-157, Iridium-192, and Cobolt-60 in practical NDT application [8]

Table 2.1 Radiation Source used in industrial radiography in average energy and HVT of lead

Gamma source	Half-life	Average Energy Level in MeV	Half value thickness in mm Lead
Cobalt-60	5.27 year	1.25	13
Cesium-137	30 year	0.66	8.4
Iridium-192	73.83 day	0.45	2.8
Selenium-75	119.77 day	0.32	2

2.5 Quantitative consideration [8]

The radiation is described mathematically based on the intensity changes during a radiographic inspection. This approach illustrates the essential factors determining the radiation contrast for the practical work.

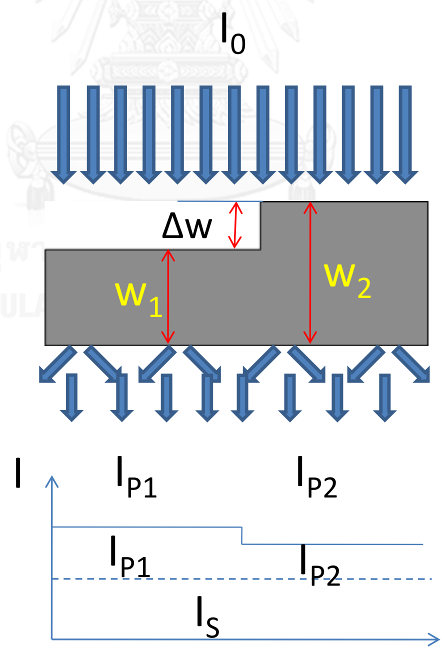

Figure 2.13 Formation of radiation contrast

The total intensity Ig behind the specimen equals the sum of the intensity of the attenuated primary beam Ip and that one of the scatter radiations I_S:

$$I_g = I_P + I_S \tag{2.7}$$

Since the scatter radiation I_S spreads out into all spatial directions it contributes homogeneously to the total everywhere directly behind the specimen as long as the difference in material thickness Δw remains small. As a consequence, the diffuse nature of the scatter radiation results in an offset intensity or basic brightness in the radiographic image as shown in figure 2.13.

The intensity difference ΔI that is of fundamental importance to enable flaw detection, since it is caused by the alterations of the penetrated wall thickness Δw, now appears simply as the difference between the intensities of the two primary beams I_{P1} und I_{P2}

$$\Delta I = I_{P1} - I_{P2} \tag{2.8}$$

When applying the law of attenuation here

$$I = I_0 \, e^{-\mu . w} \tag{2.9}$$

then a relationship can be concluded between ΔI und Δw as well as with the x-ray attenuation coefficient which is energy dependent.

This results in:

$$\Delta I \approx I_P \, . \, \mu \, . \, \Delta w \tag{2.10}$$

The relative radiation contrast K_S denotes the ratio of the intensity difference ΔI to the total intensity I_g.

$$K_S = \frac{\Delta I}{I_g} = \frac{\mu . \Delta w}{1 + \frac{I_S}{I_P}} \tag{2.11}$$

More commonly said with regard to the difference between two attenuation coefficients (e.g. μ of the specimen and μ_f of the material flaw), the radiation contrast which is fundamental for the radiographic inspection is defined as:

$$K_S = \frac{(\mu - \mu_f) . \Delta w}{1 + \frac{I_S}{I_P}} \tag{2.12}$$

In this context, the scatter ratio K is defined as: $K = \frac{I_S}{I_P}$

With I_S = scattered radiation

I_P = primary radiation

The ratio $C_S = \frac{(\mu - \mu_f)}{1 + k}$ is known as specific contrast

2.6 Intensifying Factor (IF)

Intensifying factor is the most accurate factor that measure speed of screen-film. Intensifying factor or IF is the ratio of the x-ray or gamma ray exposure needed to produce the same optical density with and without screen and expressed by the equation.

$$IF = \frac{\text{exposure required without screen}}{\text{exposure required with screen}} \tag{2.13}$$

2.7 Radiography contrast [9]

Radiography contrast ΔD corresponding to a wire of diameter d of a penetrameter placed on a plate whose thickness is T can be obtained from the following formula.

$$\Delta D = \frac{-0.434\gamma\mu\rho\sigma d}{(1+n)} \quad .(2.14)$$

Where

γ = Gradient of the tangential line at density D of x-ray film characteristic curve

$\mu\rho$ = X-ray quality when the sensitivity coefficient of the x-ray film is considered

σ = Correction coefficients by focal spot size and geometrical conditions of irradiation

n = Quotient obtained by dividing the dose rate of the scattered radiation that reaches the x-ray film uniformly multiplied by its sensitivity coefficient, by the dose rate of the penetrated radiation multiplied by its sensitivity coefficient

Therefore, once basic data on each factor is obtained, ΔD corresponding to the radiographic conditions can be obtained by calculation.

2.7.1 Film contrast [9]

Figure 2.14 show a characteristic curve of the no screen type x-ray film as an example. Assuming that γ is the gradient of a straight line that connects two points corresponding to D + 0.1 and D – 0.1, the relationship between density D and γ is as shown in figure 2.15 When the screen type x-ray film is combined with a fluorescent intensifying screen, the characteristic curve will be as shown in figure 2.16 and the relationship between the density and γ will be as show in figure 2.17.

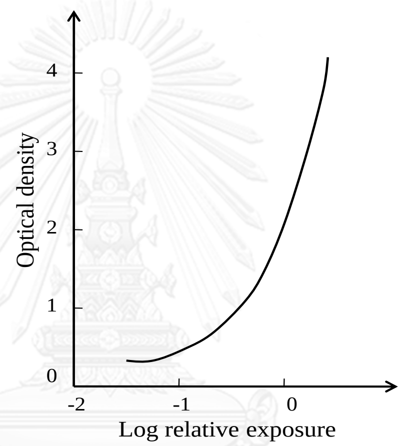

Figure 2.14 Dose characteristic curve of no-screen type x-ray film

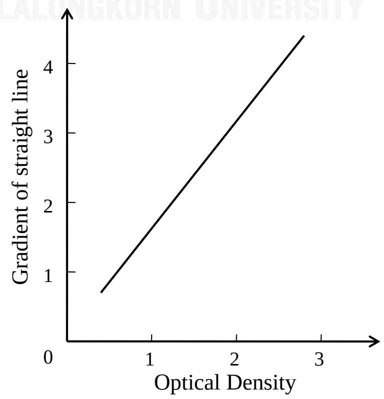

Figure 2.15 Relationship between density and gradient of straight line

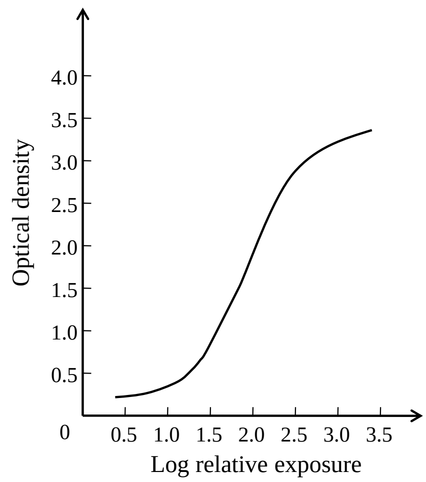

Figure 2.16 Characteristic curve of fluorescent intensifying screen type x-ray film

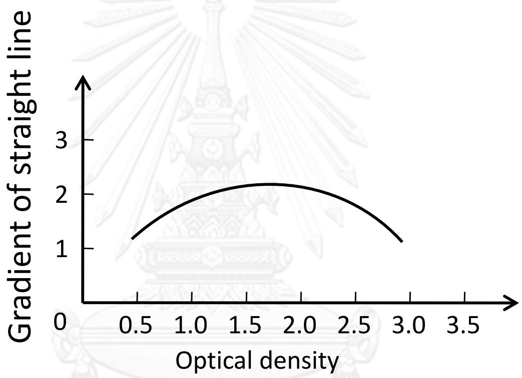

Figure 2.17 Relationship between density and gradient of straight line

2.7.2 Absorption coefficient

Absorption coefficient $\bar{\mu}$ and μ' decrease with increasing in the thickness of an absorber to be radiographed even when the tube voltage of an x-ray unit is constant, but the absorption coefficient can be regarded as nearly constant when the thickness becomes greater than a certain value. When the dose 1 mR/mA-min at a distance of 1 m which is a practical exposure condition after x-ray generate by a tube voltage quality of the penetrating radiation is expressed by μ (Fe), and the relationship between the tube voltage and μ (Fe) is shown in figure 2.18 as an example. When μ is constant, μρ can be regarded as being equal to μ even if the absorber thickness increases; with the result that μρ is eventually the same as μ Fe.

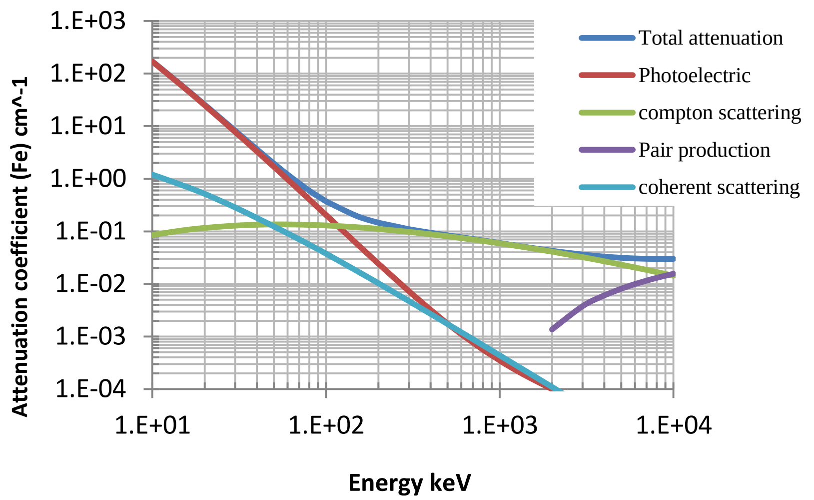

Figure 2.18 Relationship between photon energy and μ (Fe)

2.7.3 Correction coefficient

As the focal spot size f increase as against the defect size d, the image magnifying factor Mf tends to increase, but at the same time radiographic contrast of the defect is affected. Generally, the minimum perceptible contrast decrease with increase in the image width and the image becomes more easily perceptible. However, if the image is magnified when the focal spot size is large in comparison with the defect size, the value of d’ in Figure 2.19 increases. Resulting in large value of d’/d. so that the correction factor σ tends to decreases abruptly, as is evident from Figure 2.20, while radiographic contrast ΔD decrease and, consequently, the perceptibility decreases. Therefore, the geometrical requirement is such that the correction factor σ becomes nearly equal to1

When radiography is made with the arrangement shown in Figure 2.19, the apparent focal spot size d’ at the position of a wire of a penetrameter can be obtained from the following formula.

$$d' = f\ell/L \qquad (2.15)$$

Where ℓ is the distance from the center of the wire to the film, and Figure. 2.20 shows the relationship between d’d/and σ

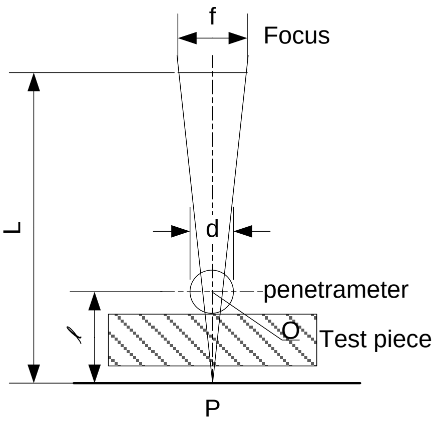

Figure 2.19 Absorption of x-ray by wire of penetrameter

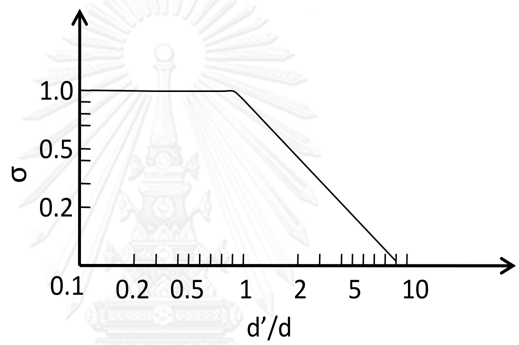

Figure 2.20 Relationship between d'/d and σ (wire)

f : Focal spot size

L: Focus-film distance

d: Wire diameter

ℓ: Penetraneter- film distance

2.7.4 Scattered direct radiation intensity ratio

Scattered direct radiation intensity ratio n can be obtained from the following formula.

$$n = \frac{(k_S I_S)}{(k_a\, I_a)} \tag{2.16}$$

where

k_S = Sensitivity coefficient of x-ray film as against quality of scattered radiation

I_S = Scattered dose rate

k_a = Sensitivity coefficient of x-ray film as against quality of penetration radiation

I_a = Penetrating dose rate

The Figure 2.21 shows the scattered direct radiation intensity ratio of SUS304 stainless steel measured by using x-ray film.

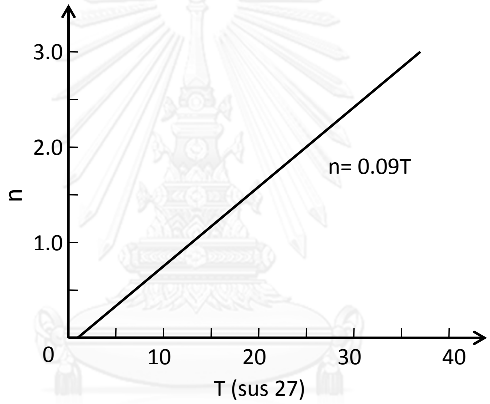

Figure 2.21 Scattered direct radiation intensity ratios when sensitivity coefficient of x-ray film is considered.

2.8 Influence of geometrical conditions [9]

Since various factors such as exposure time, photographic density, influence on the penetrometer sensitivity are related to each other in radiography, the geometrical arrangement of radiography cannot be determined in general term. Geometrical factors to be considered include the following.

2.8.1 Dimensions of focus and source

In actual radiography with x-ray, the effective focus size differs depending on the direction of the beam even in the same radiation field making is necessary to identify the size of the effective focus size in each direction of the beams when rigorous inspection is required. Regarding from the source manufacturer and its indication is used as it is.

2.8.2 Radiographic unsharpness and enlarged image due to focal spot size and geometrical arrangement

One of the influences by geometrical conditions is the radiographic unsharpness due to the focal spot size of the x-ray unit of the size of the gamma ray source. Given that the focal spot size is f, the distance between the focus and defect is L_1, the distance between the defect and x-ray film is L_2, and the size of the defect is d, the relationship between the radiographic image and geometrical arrangement as shown figure 2.22

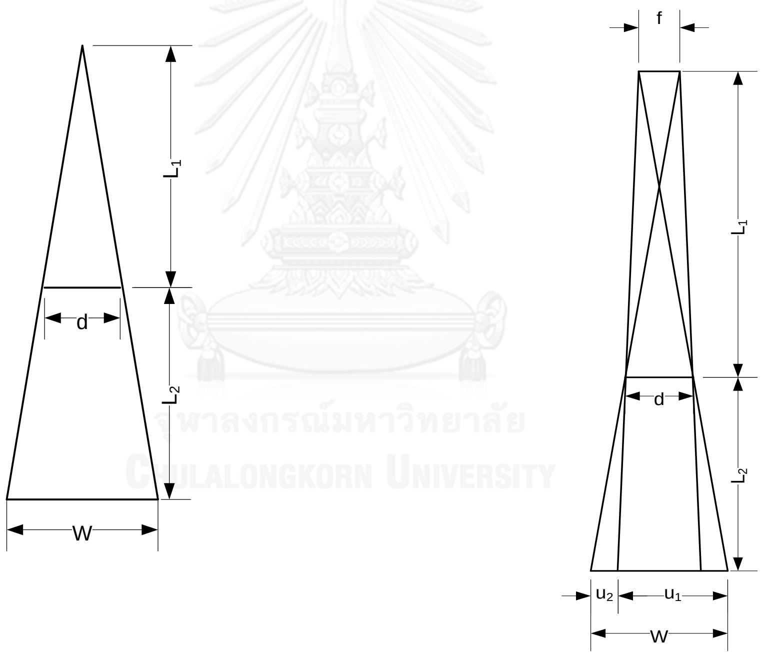

a) Enlargement of the image when the focal spot size can be ignored against the defect size

b) Enlargement of the image when the focal spot size is taken onto consideration

Figure 2.22 Influence of geometrical arrangement on radiographic image

In (a), in which the focus size is very small and is assumed to be a point, there is no penumbra of the image. In (b), in which the focus has a size of f, a penumbra is produced on the outer periphery of the image, creating geometrical unsharpness of the image. The size of this unsharpness varies with focal spot size f and the distances between focus, defect and film. Given the size of the unsharpness is μ_1, it can be obtained from the following formula.

$$\mu_1 = f\frac{L_2}{L_1} \tag{2.17}$$

As can be seen from figure 2.22, the size of defect image w is magnified more than the size of defect d. figure 2.22 is a case in which f is regarded as a point. Given the magnifying factor at that time is m_0, it can be obtained from the following formula.

$$m_0 = \frac{w}{d} = \frac{L_1 + L_2}{L_1} \tag{2.18}$$

When the focal spot size is f as in figure 2.22 (b), defect image w is $\mu_1+\mu_2$. Hear, μ_2 can be obtained from the following formula.

$$\mu_1 = d \times \frac{L_1 \times L_2}{L_1} \tag{2.19}$$

Therefore,

$$w = \left(f \times \frac{L_1}{L_2}\right) + \left(d \times \frac{L_1 \times L_2}{L_1}\right) \tag{2.20}$$

Here, given the magnifying factor at this time is mf, the following formula derive.

$$mf = \frac{w}{d} = \frac{f}{d} \times \left(\frac{L_1}{L_2} + \frac{L_1 + L_2}{L_1}\right) \tag{2.21}$$

$$mf = m_0\left(\frac{f}{d} + 1\right) - \frac{f}{d} \tag{2.22}$$

However, the magnifying factor in this case involes the geometrical unsharpness of the image, and the greater the magnifying factor of the image mf, the less perceptible the image. Figure 2.23 shows the magnifying factor Mf with respect to different values of f/d, using magnifying factor m_0 as a parameter when the focal spot size is such a small point as can be ignored. Therefore, the smaller the size of defect d, the more the image tends to be magnified even with the same geometrical arrangement.

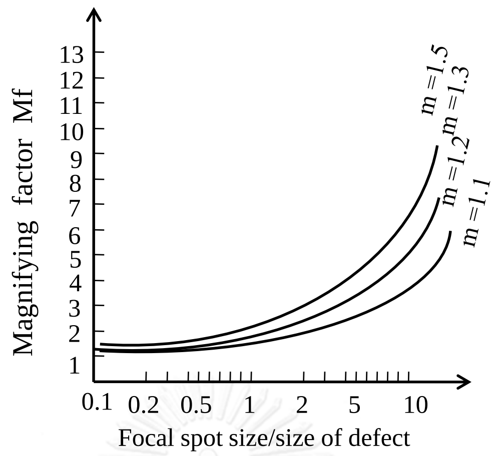

Figure 2.23 Magnifying factor Mf when focal spot size is taken into consideration

2.9 Image Quality Indicator (IQI) [8]

2.9.1 Wire type IQI

The question how good or poor is an x-ray image can be answered by referring to an Image Quality Indicator (IQI Value). To determine the IQI value, one way is to attach e.g. wire IQIs according to EN 462-1 and ISO 19232-1 at the specimen so both will appear on the image. The diameter of the wires decreases in a geometric sequence from 3.2 mm (wire W1) down to 0.05 mm (wire W19). The number of the thinnest just perceivable wire represents the image quality value. The wire is supposed to be made out of the same material as the inspected specimen. Rather frequently and particularly in radioscopic applications the image quality of an x-ray image is rated by a so-called relative wire perceptibility or testing sensitivity.

This means that the ratio of the wire diameter over the penetrated wall thickness is calculated and expressed in percent by the equations.

$$\%\ \text{sensitivity} = \frac{\text{Diameter of smallest vissible wire}}{\text{Thickness of specimens}} \times 100 \qquad (2.23)$$

A wire diameter of 1mm on a 100 mm thick wall thus results in a wire perceptibility of 1%.

Figure 2.24 Wire DIN IQI according to EN 462-1 (and ISO 19232-1) each size composes of 7 wires, place parallel 5 mm distance from each other [8]

Table 2.2 Diameter of wire DIN IQI according to EN 462-1

Diameter (mm)	3.20	2.50	2.00	1.60	1.25	1.00	0.80	0.63	0.50	0.40
Wire No.	1	2	3	4	5	6	7	8	9	10
Diameter (mm)	0.32	0.25	0.20	0.16	0.125	0.10	0.08	0.063	0.05	
Wire No.	11	12	13	14	15	16	17	18	19	

2.9.2 Contrast sensitivity IQI

Figure 2.25 represents the scheme of the ASTM E 1647 IQI which is designed for measurement of the contrast sensitivity of unsharp radioscopic systems. It is also included in the phantom IQI of EN 14784-1 and ASTM E 2445 for long term stability check in computed radiography. It consists of a metal plate of given thickness and material. Four milled squares are in the material with 1, 2, 3, 4 % depth of the IQI block. The operator can evaluate the contrast sensitivity by visual evaluation of the number of visible squares.

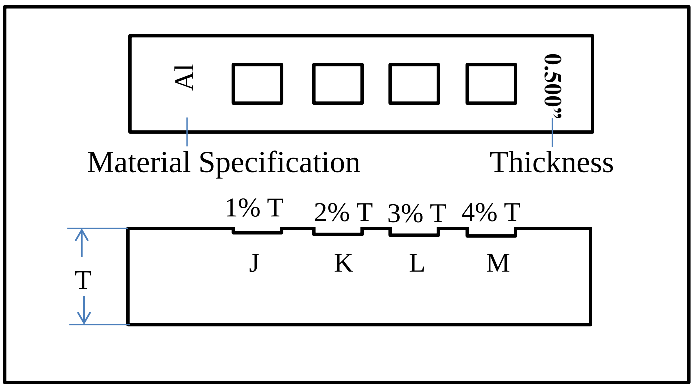

Figure 2.25 Contrast sensitivity gage in accordance with ASTM E 1647 [8]

2.9.3 Platinum duplex wire IQI (EN 462-5, ASTM E 2002, ISO 19232-5)

The duplex wire IQI system consists of a series of 13 elements. Each element consists of a pair of wires with a circular diameter. The distance between the wires of each pair is equivalent to their diameters. The elements are cast into a rigid block of plastics as shown in the figure 2.26.

The pair of wires which just cannot be resolved as such in the image is regarded as the indication of the limit of what can be distinguished. Then the image unsharpness is given by the double of the wire diameter. This image quality indicator suits for determination of the unsharpness only and therefore should be applied only in conjunction with wire IQIs or the plaque systems for sensitivity measurement. In order to determine the total unsharpness of a system the duplex IQI is fixed onto the specimen on the side toward the radiation source. When determining the internal unsharpness of the detector the duplex IQI is positioned directly on the detector surface.

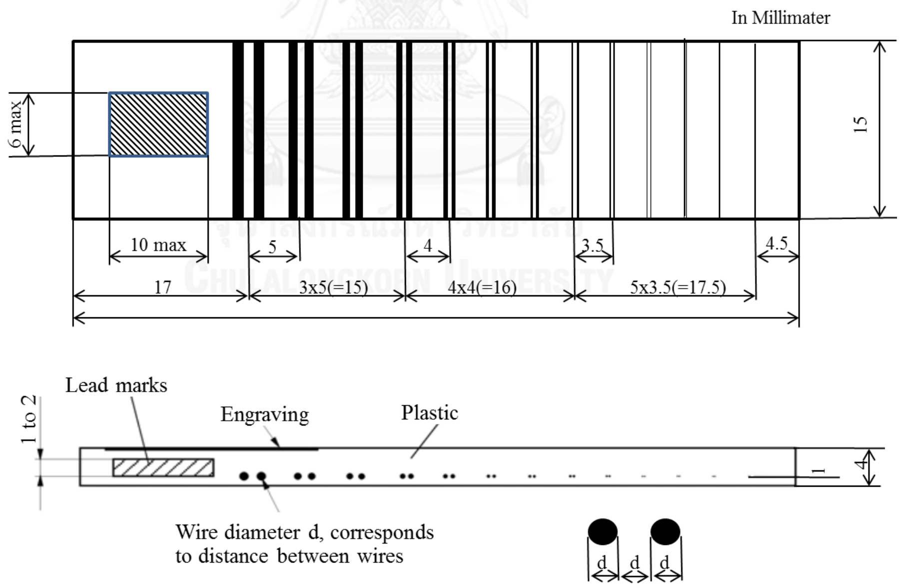

Figure 2.26 Duplex wire IQI for determination of unsharpness and basic spatial resolution in accordance with EN 462-5, ASTM E 2002, ISO 19232-5 [8]

2.10 Advantage and weakness of the conventional film radiographic technique

In present, the digital radiography technology is developed to be high sensitivity and high resolution system and able to be the real time inspection. And also, the high performance detector and developed control software make the digital technology is more convenient for user. However, the conventional film radiographic technique is continually popular technology, especially for the industrial field. The advantages and weaknesses of the conventional film radiographic technique are listed below.

2.10.1 Advantage of conventional film radiographic technique

- The standard procedure of the conventional film radiographic technique is widely published for the routine inspection.

- The method provides the permanent record which is best for the reliability from the view point of inspection.

- Most material can be inspected and dose not required the smooth surface of specimens for example not removing the insulation of object, moreover, can be applied in high temperature environment.

- High image quality, especially for the image resolution compare with the digital recorder. The resolution can be less to 0.8 micron due to the grain size of silver emulsion for Agfa and Kodak x-ray film [10].

2.10.2 Weakness of conventional film radiographic technique

- The chemical processing is needed to produce the radiographic image. The low chemical quality can cause the low image quality.

- The appropriate exposure time should be taken in the linear range of the film characteristic curve to obtain the most object information from the high contrast condition.

- Low efficiency, the result from experiment was obtained the percent absorption of industrial film high speed Kodak AA400 with the gamma ray at 316 keV of and 1332 keV of Co-60, 0.3% and 0.16% respectively. Therefore, in case of thick sample, the high energy radiation with long exposure time is needed to produce the good image quality.

- The specimen must be suitable for the Geometry of film replacement and radiation source which must be place on each size of specimen

- The cost-loss from the trial and error can be occurred, particularly for an unknown object especially specimens from archeology.

- Required radiation safety officer for operate the radiography

- The thickness of specimen for radiographic technique depend on energy of radiation source shown in table 2.4

Table 2.3 Radiation source for different specimens thickness [11-13]

Radiation Source	Approximate limit Thickness (mm)	
	Concrete	Steel or equivalent
X-ray 150 keV	-	25
X-ray 300 keV	-	76.2
X-ray 400 keV	-	88.9
Ir-192	250	76.2
Co-60	500	203
X-ray 18 MeV, Linac	1600	500

2.11 Literature review

In 1998, Bulubay U., et al. [1] studied and evaluated the quantitative results of intensifying screens for increasing image quality of Co-60 radiography. Steel, copper, cadmium, indium, gadolinium, dysprosium, gold and lead were selected as intensifying screen and placed on the front side of film. Lead screen with thickness of 0.125 mm was used as a back screen. The experiments have been carried out using same exposure for six different thicknesses of steel specimen. The penetrometers, DIN 54 109 Fe, and a special design square wave parts were used for calculation of sensitivity and MTF, respectively, and the resolution was evaluated from the frequency. In this research, the intensifying rate and resolution were mainly investigated for the comparative study. In addition, the cost of material was also considered. The results of film densities and intensifying rates showed that 127 mm-thick of specimen supplied appropriate conditions for the film. From the evaluated results of intensifying rate and resolution, dysprosium provided highest intensifying rate and copper performed good resolution. By considering the weighted mean value including cost, dysprosium is the first and steel is the last for this study.

In 1998, Lopes R.T., et al.[2] Lopes R.T., et al. studied the secondary x-rays from radiographic intensifying screens which aimed to reduce the radiation dose in radiology. The fluorescent intensifying screens were used to produce visible light for increasing efficiency of the x-ray film. The fluorescent screen consisted of Gd_20_2Si: Tb with the thickness of 9.09×10^{-2} g/cm^2 and 1.55×10^{-1} g/cm^2 for the front and back screens, respectively. An Am-241 with 240 mCi was used as a gamma ray radiation source which emitting energy of 59.54 keV. The intensities of the primary and secondary radiation were measured with angular distribution. The results showed that the scattering radiation intensities consisting of Rayleigh and Compton scattering were high at small angle (<30°). And the intensities were decreased at 90° due to the absorption from crossing a large path inside the screen. The ratio of secondary-to-primary radiation on x-ray film for front screen was 7.7% and for back screen was 8.0%. Therefore, the ratio of secondary-to-primary radiation on x-ray film was 16%. Moreover, the x-ray fluorescence of Gd in screen and the secondary radiation can affect the image resolution..

In 1997, Kandarakis I., et al. studied the performance of scintillator employed in radiation detector of medical imaging system and they present the method to determine the spatial-frequency-dependent detective quantum efficiency (DQE) of scintillators independently of the optical detector. The DQE was determined in terms of its luminescence efficiency (LE), quantum detection efficiency (QDE), modulation transfer function (MTF) and light emission spectrum. Various scintillator types, Gd_2O_2D:Tb, La_2O_2S:Tb, Y_2O_2S:Tb and Zn_2Cd_2:Ag with the thickness of 50, 80 and 120 mg/cm^2 for each screen were prepared for comparison. The medical x-ray tube was employed to excite the scintillators at 90 kVp. The results of LE values showed the Gd_2O_2D:Tb screen was most efficient followed by La_2O_2S:Tb, Zn_2Cd_2:Ag and Y_2O_2S:Tb screens, respectively. For Gd_2O_2D:Tb screen, the LE decreased at thick screen of 120 mg/cm^2 but the LE of other screens seem to be saturated. The QDE of Gd_2O_2D:Tb screen was varied from 0.41-0.66 and La_2O_2S:Tb screen was varied from 0.23 to 0.46. By measuring the emission spectra of scintillators, all spectra were presented in the green region of the visible light spectrum. From this study, the DQE values were varied between 0.13-0.33 depending on the scintillator material, the coating weight of screen and the operating voltage of x-ray tube. The Gd_2O_2D:Tb screen show the highest DQE which the condition was maintained at frequencies up to 100 cycles/cm. Moreover, the DQE of thin screens was found to be higher than the thicker one at the same material.

In 1990, Zananiri F.A.F. et al. [4] Presented evidence of the dual energy radiography using x-ray film and intensifying screen. The aim of this study was to investigate dual energy (DE) systems using x-ray films and intensifying screens as detecting media. This has been studied using both experimental methods and numerical mode. Numerical methods were used to calculate energy losses due to K-fluorescent escape originating from the phosphors of the intensifying screens. This enabled the calculation of absorbed energy in screens. It method for screen selection and prediction of performance used the fact that detector response depends upon impinging x-ray energy. By equating the detector's absorbing characteristics to the resultant optical density (OD), an absorbed energy constant was calculated. These constants were used to predict OD for a given x-ray spectrum and hence simulation of detector characteristics. Experimental techniques were used to investigate sensitivity to chemical composition changes. These results compared favorably with computed values. It was demonstrated that although limitations exist, detector simulations are valid and x-ray film intensifying screen combinations make adequate DE detectors.

In 2003, Feyzi I., et al. [14] investigated the impact of lead oxide screen on the image formation by using Monte Carlo simulation and also general trends. The objective is to increase the efficiency of the energy deposition into the film. For the simulation, the intensifying screen was PbO which composed of 7.17% of oxygen and 92.83 % of lead. The density was 11.35 g/cm^3. The thickness of PbO screen and x-ray energy were varied for understanding the mechanism of photon and electron interactions with matter as a function of energy. From the study of energy spectrum of incident photon, it showed that uncollided and scattered photons did not attribute some other functions to the intensifying screen. Moreover, the computation results showed that the detection efficiency is much better at the low energy around 50 keV. At higher energy, the detection efficiency decreased significantly. As the thickness is increased further, intensifying screen came to be a filter rather than an intensifying screen. At last, the results can be concluded that screen thicknesses can be increased to 3 mm. for photon energy around 500 keV and to 5 mm. for 7000 keV.

CHAPTER 3
MATERIAL AND EXPERIMENTAL

Chapter 3 explains equipment, materials and radiographic technique as well as the developed methods and device in this study. The methods are mainly separated to 4 parts; the first part introduces the radiographic system, equipment and materials e.g. types of radioisotope source, film type, intensifying screens, which are used to conduct this research. The second part describes methodology of the conventional film radiographic technique compared with the developed method using various intensifying screens. The main purposes are to investigate the properties of intensifying screen and to develop technique for improving the speed of film radiography. The methods employed in determining radiographic speed and image quality are also described. The third part describes application of the developed method to radiograph the test specimens. The last part describes the design and construction of the new technique and device for determining the exposure time for gamma radiography using film which is useful for any test specimens. The equipment and methods are explained below.

3.1 Industrial radiographic equipment

3.1.1 Radioisotope source

This research was conducted with the radioisotope sources including Iridium-192 and Cobolt-60 which are typically used in the industrial radiography. Ir-192 has a half-life of 73.8 days and gives off multi-energy gamma-rays with the average energy of about 300 keV. Co-60 has a half-life 5.27 years and gives off gamma-rays with the average energy of 1.25 MeV. The two sources are 6 Ci Ir-192 of the Thai Non-destructive Testing Public Company Limited and 10 Ci Co-60 of the Non-Destructive Testing Division of Thailand Institute of Nuclear Technology (public Organization). The radioisotope sources Ir-192 and Co-60 are shown in figure 3.1(a) and 3.1(b), respectively.

(a) (b)

Figure 3.1 Gamma projector of Ir-192 radioisotope source (a) and gamma projector of the Co-60 radioisotope source (b)

3.1.2 X-ray generator

The model RF-200EGM2 of x-ray generator manufactured by RIGAKU is used in this research. The x-ray tube voltage can be varied from 70 kVp to 200 kVp. The tube current can be operated with two modes, the STD mode provides current of 5 mA and the LOW mode provides lower current of 4 mA. The x-ray focal spot size is 2 mm × 2 mm. The illustration of the x-ray tube and the x-ray generator control unit are shown in figure 3.2(a) and 3.2(b), respectively.

(a) (b)

Figure 3.2 X-ray generator tube of RIGAKU model RF-200EGM2 (a) and the control unit (b)

3.1.3 Film

Film is widely used as image recorder of radiographic technique for non-destructive testing in industry. Typically, the radiographic film types can be mainly separated to two categories which are the direct exposure film or non-screen film and the indirect-exposure film for use with the intensifying screen.

In this research, a high speed and high contrast film type, Kodak Industrex AA400 was selected due to its appropriate properties and can be used for both direct radiography and with lead screen. It is also widely used in industrial radiography. The relative exposure factor (inversion of the film speed) of Kodak AA400 is compared with the other Kodak film types as shown in table 3.1. It should be noted that the relative exposure was determined based on the optical density of 2.0 of radiograph in controlled condition of standard manual film development of 4 minute at 20^{o} C. The characteristics of Kodak AA400, exposure curve and its spectral sensitivity are shown in figure 3.3 and figure 3.4, respectively.

Table 3.1 Relative exposure for various energy level of Kodak Industrex film [15]

Kodak INDUSTREX Film	Relative Exposure for various energy level			
	ISO 120 kV[1]	En 220 kV[2]	Iridium192[3]	Cobalt 60[4]
INDUSTREX DR50	9.0	7.2	9.0	9.0
INDUSTREX M100	4.1	4.2	5.4	6.3
INDUSTREX MX125	2.9	2.8	3.1	3.3
INDUSTREX T200	1.6	1.7	1.9	1.9
INDUSTREX AA400	1.0	1.0	1.0	1.0
INDUSTREX HS800	-	0.5	-	-

1. In accordance with ANSI PH2.8-ISO 7004 standard without lead screen
2. In accordance with ANSI PH2.8-ISO 7004 standard EN ISO11699-1. Lead screen
3. 8 mm copper filtration 100/200 micron lead screen
4. 100/200 micron lead screen

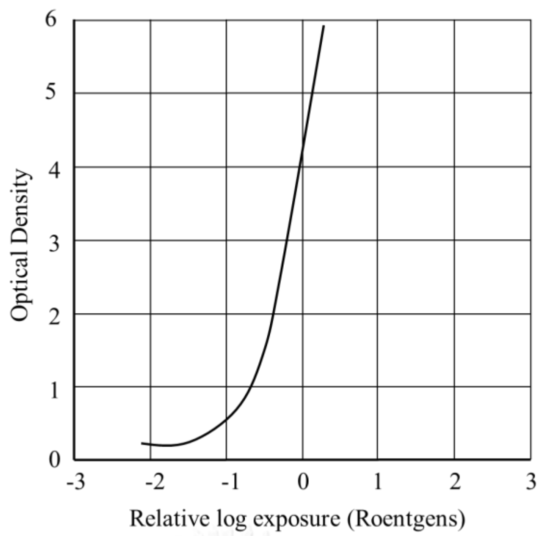

Figure 3.3 Film exposure curve of Kodak Industrex AA400 [13]

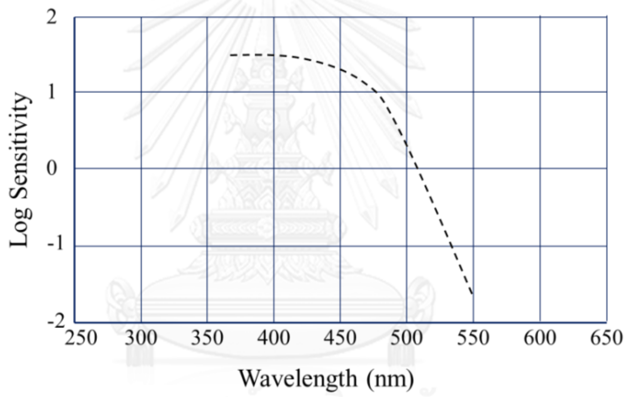

Figure 3.4 Film sensitivity of Kodak Industrex AA 400 [13]

3.1.4 Intensifying screens

The radiographic image is formed by only approximately 1 % of the amount of radiation exposed to the film. To obtain higher recording efficiency of the film, it should be sandwiched between two intensifying screens. For this research, the conventional lead screen and dysprosium (Dy) metallic screen as well as fluorescent screens including PI-200, DRZ and Blue 800 screens were used.

3.1.4.1 Lead screen

Lead screen is the intensifying screen which is generally used to enhance the sensitivity of radiograph for the conventional technique. For the experimental setup, film was sandwiched with two lead screens. The first screen (top screen) with a thickness of 0.005 inch was placed on top of the film on the source side and the other (back screen) with a thickness of 0.010 inch was placed behind the film.

3.1.4.2 Dysprosium screen

Dysprosium is a rare earth element that has a metallic bright a silver luster. It is commonly used in the neutron radiography using transfer technique, dysprosium was used for neutron converter screen which high absorption cross section for neutron. According to literature review, dysprosium was used for Co-60 high gamma radiation and high intensifying rate. For experiment setup, film was sandwiched with two dysprosium sheet of 0.5mm thickness.

3.1.4.3 PI-200 fluorescent screen

PI-200 is a terbium-activated gadolinium oxysulfide (Gd_2O_2S:Tb) fluorescent screens manufactured by Mitsubishi Chemical Corporation. PI-200 screen has high thickness of phosphor layer which results in high energy absorption and brightness for MeV radiography. The specifications of the PI-200 fluorescent screen is shown in table 3.2.

Table 3.2 Intensifying screen PI-200 specification [16]

Name	Composition		Relative Brightness*[1]	MTF*[2]	
				at 1 Lp/mm	at 2 Lp/mm
PI-200 (Gd_2O_2S:Tb)	Protective Layer	PET 6um	122%	0.35	0.11
	Phosphor Layer	436um, 200mg/cm2		-80	-70
	Supporting Layer	Plastic Base 188um			
	Total	630um			
ref. DRZ-HIGH (Gd_2O_2S:Tb)	Protective Layer	PET 9um	100%	0.44	0.16
	Phosphor Layer	310um, 145mg/cm2		-100	-100
	Supporting Layer	Plastic Base 188um			
	Total	507um			

Condition
*1 X-ray: 300 keV , Film: Fuji UM-MA HC (single emulsion type)
*2 X-ray: 80 keV, Lead test pattern: Kyokko type 7, Film: Fuji MU-MA HC (single emulsion type)

3.1.4.4 DRZ-std fluorescent screen

DRZ screen is also a Gd_2O_2S:Tb fluorescent screens manufactured by Mitsubishi Chemical Corporation which is used for indirect conversion radiography. Indirect systems using Gd_2O_2S:Tb have advantages of heightened stability, improved safety, lower cost and minimized environmental impact. DRZ screen can be categorizes to three types and specification of DRZ screens are shown in table 3.3.

DZR-Std : Highest resolution composed of a double layer structure

DRZ-Plus : A valance of high brightness and resolution with a double layer structure

DRZ-High : Superior Brightness

Table 3.3 Specifications of DRZ fluorescent screens [16]

Name	Composition		X-ray*1 Attenuation	Brightness*2 [cd m-2/R sec-1]	Relative Brightness	MTF*3	
						at 1 Lp/mm	at 2 Lp/mm
DRZ-STD (Gd2O2S:Tb)	Protective Layer	PET 6um	42%	17	145%	0.82	0.49
	Phosphor Layer	140um, 68mg/cm2				-106	-114
	Supporting Layer	Plastic Base 250um					
	Total	406um					
DRZ-PLUS (Gd2O2S:Tb)	Protective Layer	PET 6um	53%	85	173%	0.72	0.36
	Phosphor Layer	208um, 100mg/cm2				-93	-83
	Supporting Layer	Plastic Base 250um					
	Total	464um					
DRZ-HIGH (Gd2O2S:Tb)	Protective Layer	PET 9um	66%	11.2	229%	0.44	0.16
	Phosphor Layer	310um, 145mg/cm2				-57	-37
	Supporting Layer	Plastic Base 188um					
	Total	507um					
Competitor´s product Regular Type (single screen)	Total	380um	40%	4.9	100%	0.77 -100	0.43 -100
Competitor´s product Regular Type (single screen)	Total	550um	62%	7.7	158%	0.61 -79	0.26 -61

Conditions;
*1 X-ray: 80kV, Water 100mm (Tube side), Dose measurement: Victoreen Model 500
*2 X-ray: 80kV, no Phantom Brightness measurement: TOPCON Luminance Colorimeter BM-5A Dose measurement: RTI Electronics Solidose 300
*3 X-ray: 80kV, Phontom: Water 100mm (Tube side), Lead Test Pattern: KYOKKO Type 7 (Pb 0.10mm) x-ray film: Fuji UM-MA HC (single emulsion type)
For this research DRZ-std screen type were conducted the experiment.

3.1.4.5 Blue 800 fluorescent screen

The Blue 800 speed rare Earth x-ray screen manufactured by Penn-Jersey x-ray. It composes of rare earth, barium fluorobromide which is an active radiation phosphor component [17]. The blue 800 fluorescent screen can emits the spectrum of light in wavelength of blue and ultraviolet, therefore this screen is compatible with blue sensitive film.

Figure 3.5 Blue 800 fluorescent screen

3.1.5 Steel step wedge

Steel step wedge was used as a standard specimen to create the exposure curve plotted between the optical film density and the steel thickness. The thicknesses of steel are 5.48, 6.89, 8.14, 10.72, 11.15, 12.79, 14.3, 16.6, 18.1, 20, 21.06, 22.56, 24, and 25.33 mm, respectively. The illustration of the steel step wedge is shown in figure 3.6

Figure 3.6 Steel step wedge

3.1.6 Densitometer

Densitometer model of PDA-81 manufactured by KONICA Corporation was used to measure the light transmission from the obtained radiographic film compared with the original light intensity, which is namely the optical density. The optical density is in range of 0.0-4.0 can be read out from 3-mm diameter of measuring area.

The wave length of light source must be within visible light. The illustration of densitometer is shown in figure 3.7.

Figure 3.7 PDA-81 densitometer from KONICA Corporation

3.1.7 Image Quality Indicator (IQI)

Wire type of image quality indicator DIN IQI EN 462-1 was used in this research to investigate the image quality from radiographic film. The European standard IQI EN 462-1 composes of 3 sets of steel wires as shown in figure 3.8 and the IQI details are described below;

- IQI set 1(1 FE DIN) containing W1 to W7, the wire diameters are 3.2, 2.5, 2.0, 1.6, 1.25, 1.0, and 0.8 mm, respectively
- IQI set 2(6 FE DIN) containing W6 to W12, the wire diameters are 1.0, 0.8, 0.63, 0.5, 0.4 0.32, and 0.25 mm, respectively
- IQI set 3(10 FE DIN) containing W10 to W16, the wire diameters are 0.4, 0.32, 0.25, 0.2, 0.16, 0.125, and 0.1 mm, respectively

Figure 3.8 Image Quality Indicator DIN IQI EN642-1

3.2 Methodology for improvement of speed of conventional film radiographic technique and determination of quality of screen-film image.

3.2.1 Investigation of Intensifying Factor (IF) of intensifying screen

3.2.1.1 Intensifying factor of metal screen

U. Bulubay et al. 's work [1] studied and determined the quality of various intensifying screens to increase the image quality for Co-60 radiography by using a metallic intensifying screen as the front screen and a 0.152-mm lead sheet as the back screen. They concluded that the dysprosium screen provided the highest intensifying rate. In this research, however, two types of metallic screen were used as the back screen to determine the intensifying factor for Co-60 radiography. The experimental equipment and conditions are listed below:

- Co-60 radiation source
- Kodak AA400 film
- Dysprosium and lead screen
- Source to film distance is 80 cm
- Film processing: 5 min-developing time and 5 min-fixing time, consequently, at the room temperature

Dysprosium and lead screens were placed on the back side of film and were exposed simultaneously by varying the exposure from 4.7-7.6 Ci-min of Co-60. The Kodak AA400 film without metallic screen was also exposed at the same condition for comparison. Intensifying factor could then be calculated from readout of film optical density with and without metallic screen. Figure 3.9 shows the schematic setup of the experiment for comparison of Pb and Dy screens.

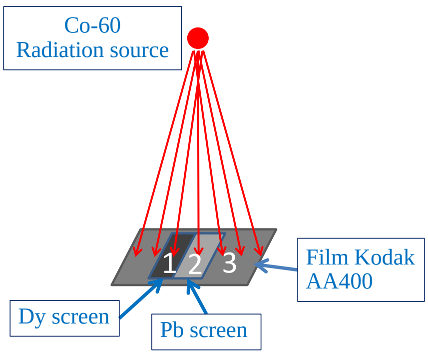

Figure 3.9 Schematic setup of the experiments for comparison of Pb and Dy screens

3.2.1.2 Intensifying factor of the fluorescent screens

Various types of intensifying screen including the PI-200 screen, the DRZ-std screen, the Blue screen and the conventional lead screen were tested to compare the screen intensifying factors. The two type radiation sources, gamma ray radioisotope and x-ray generator, were used with varying exposures (Ci-min. for gamma-rays and mA-min. for x-rays). The kilovoltage settings of x-ray generator were 100 kVp, 130 kVp, and 160 kVp, respectively.

The source to film distance was fixed at 80 cm. The condition of film processing was 5 minute for film development and 5 minute for film fixing at room temperature. The intensifying factor of image could be determined from the optical film density using the densitometer at the optical film density of 2.0. The optical film density with and without the screens were then compared.

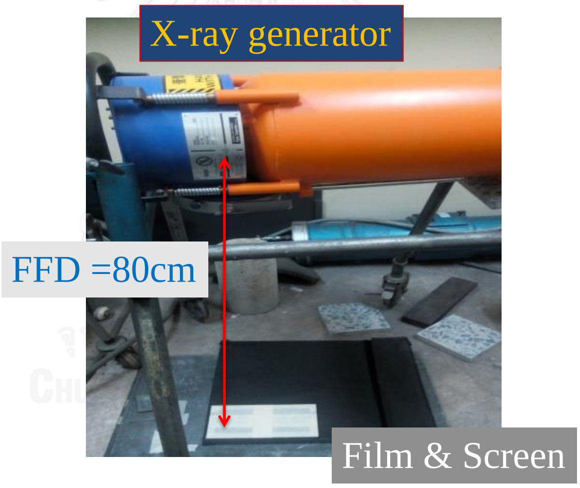

Figure 3.10 Experiment setup of the intensifying factor of film radiography with fluorescent screen by using x-ray generator

To determine the intensifying factor, the characteristic curve of each screen-film pair must be plotted between the optical film density and the log relative exposure then fitted with the exponential function. The log relative exposures at the optical density of 2.0 of each screen-film pair and of the bare film (without intensifying screen) were obtained from the curves. The difference between the log relative exposures of each screen-film pair and the bare film was used to calculate the intensifying factor. The Intensifying factor could be easily obtained from antilog of the difference.

3.2.2 Investigation of the quality of screen-film radiography

3.2.2.1 Scattered radiation effect testing

In x-ray and gamma-ray radiography, film records not only the direct transmitted radiation but also the scattered radiation from the specimen. The scattered intensity increases with increasing of the specimen thickness and decreases with increasing of atomic number of the specimen. Concrete specimen, for example, gives high scattered intensity due to its composition and thickness. The scattered photons would diminish contrast and definition (sharpness) of the radiographic image. Since the scattered photons have lower energy than the direct transmitted photons, they can be partly cut-off to prevent them from reaching the film. In this study, we have investigated the effect of scattered radiation from the peak to Compton ratio of gamma-ray spectra from concrete specimens of varying thicknesses. A NaI(Tl) detector with lead collimator was used to measure Co-60 gamma-ray spectra passing through concrete specimens having thicknesses between 0-20 cm. The obtained spectra were used to determine the ratio of the photopeak intensity to the Compton continuum intensity. The experimental setup is shown in figure 3.11.

3.2.2.2 Reducing of scattered radiation using lead filter

To eliminate part of the scattered radiation to improve the image quality, lead sheet was applied as the filter. In this study, the lead sheet was inserted between specimen and detector. According to the previous experiment, 10 cm-thickness concrete caused the highest scattering fraction. The Co-60 gamma-ray spectra were collected at varying lead sheet thicknesses from 1 to 8 mm. Fraction of the scattered radiation intensity was calculated at each filter thickness and plotted as function of the lead sheet thickness.

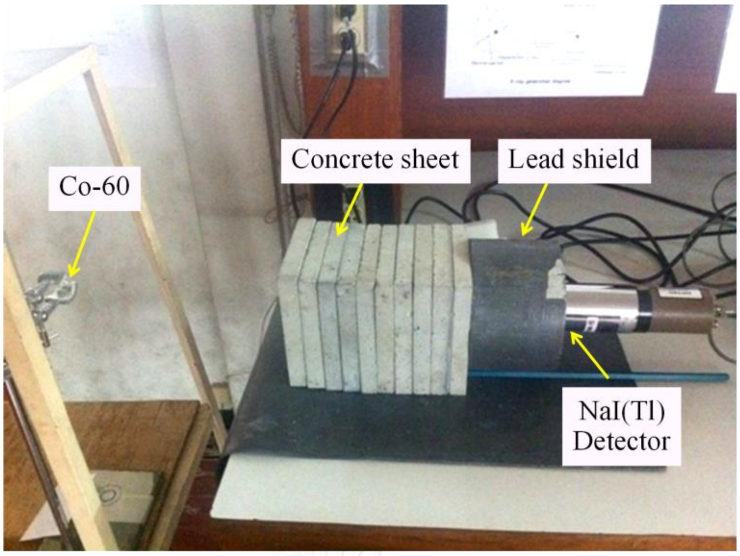

Figure 3.11 Experimental setup to determine peak to Compton ratio

3.2.2.3 Image contrast of each screen-film type

This purpose of this experiment is to investigate the image contrast of various screen-film pairs. The films were tested with different types of intensifying screen including PI-200 screen, DRZ-STD screen, Blue screen, and lead screen to compare the image quality for low energy gamma-rays from Ir-192 and high energy gamma-rays from Co-60 with varying exposures between 0.5-30 minute. The radiographic films were then processed the same condition asin the previous steps. The image contrast was determined from the slope of the film characteristic curve at the optimum optical density.

3.2.2.4 Sensitivity of screen-film radiography

Radiographic sensitivity is one of the factors to compare quality of the radiographic technique. In this study, the Image Quality Indicator DIN IQI steel wire type set 1 and set 2 were used to evaluate the sensitivity. Both sets of wire type IQIs were placed on top of the tested specimen during exposure so that the sensitivity could be determined from the smallest visible wire.

3.2.2.4.1 Sensitivity of the screen-film radiography using -ray generator

The purpose of this experiment is to investigate the image sensitivity of screen-film pairs using x-ray generator. Various types of intensifying screen were tested including the PI-200 screen, the Blue screen and the conventional lead screen. Only Kodak AA 400 industrial radiographic film was employed. Each screen-film pair was radiographed by x-rays at 100 kVp, 130 kVp and 160 kVp, respectively. The same as the previous experiments, the wire type IQIs were placed on top of the 2 cm-steel specimen for determination of the radiographic sensitivity. The radiographic sensitivity was determined at the optimum optical density of 2.0. To obtain the optical density of 2.0, the exposure for each type of screen and kV setting of the x-ray generator was determined from the previous experiment on testing of intensifying screens. The exposures for the three intensifying screens at different kV settings are shown in table 3.4

Table 3.4 Exposure of screen for each voltage of x-ray generator

Type of intensifying screen	Exposure at OD =2.0 (mA-sec)		
	100 kVp	130 kVp	160 kVp
PI-200 screen	190	465	2223
Blue screen	89	165	1012
Lead screen	48	81	531

3.2.2.4.2 Sensitivity of the screen-film radiography using radioisotope source

To determine the radiographic sensitivity, two types of specimen were tested. The first specimen was a steel plate with thickness of 2 cm. The other was a concrete block having thickness of 15 cm with 2 cm-diameter steel rod inside. The experimental setup is shown in figure 3.12 and 3.13, respectively. The wire type IQIs were placed on the test during exposure form gamma-rays from Ir-192 source. After film processing as in the previous steps, the radiographic sensitivity was obtained from the smallest visible wire on each radiograph. To avoid human factor, the smallest visible wire was determined by using the freely available Image J software.

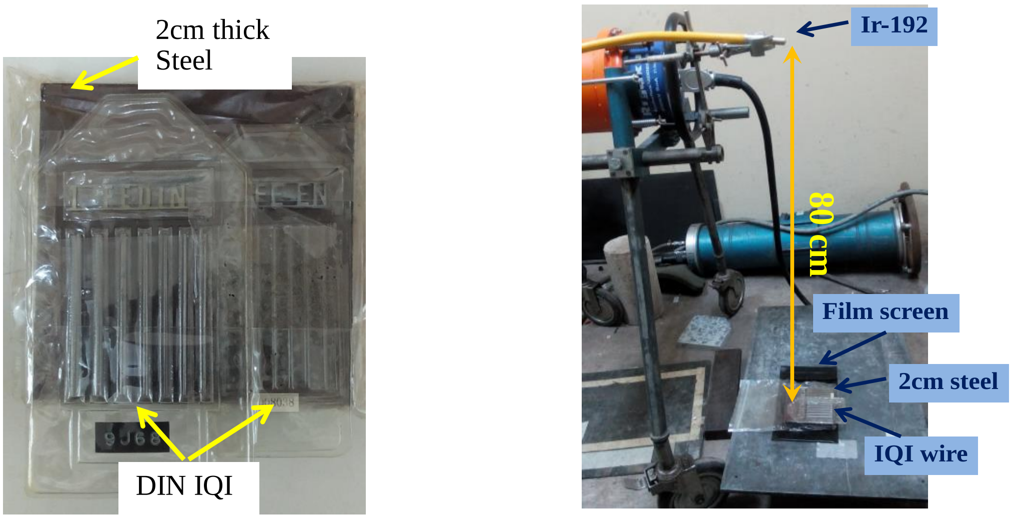

(a) (b)

Figure 3.12 Wire type IQIs wire place on top of the 2 cm steel specimen (a) and the geometry of experiment for determine the sensitivity show in (b)

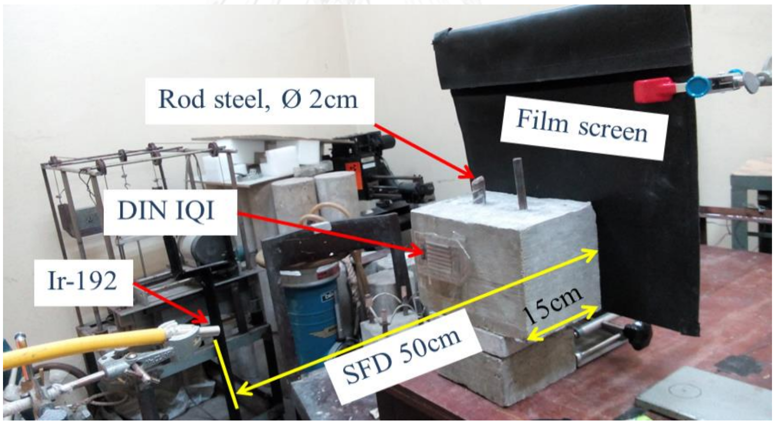

Figure 3.13 Experimental setup for investigates the image sensitivity from steel rod inside the concrete block specimen

3.3 Testing of the developed technique with thick specimens containing light elements

3.3.1 Inspection of a concrete pole structure

The aim of this study was to inspect internal structure of a concrete pole by using the developed radiographic technique in comparison to the conventional industrial lead screen-film radiographic technique. The concrete pole was inside the room 303 of the Nuclear Engineering building, Chulalongkorn University. The apparent size of the pole was 17 cm × 17 cm x 3 m. The concrete pole was radiographed with gamma-rays from an Ir-192 radiographic source using the PI200 screen-Kodak AA400 film with and without lead filter, and the lead screen-Kodak AA400 film. The experimental setup is shown in figure 3.14.

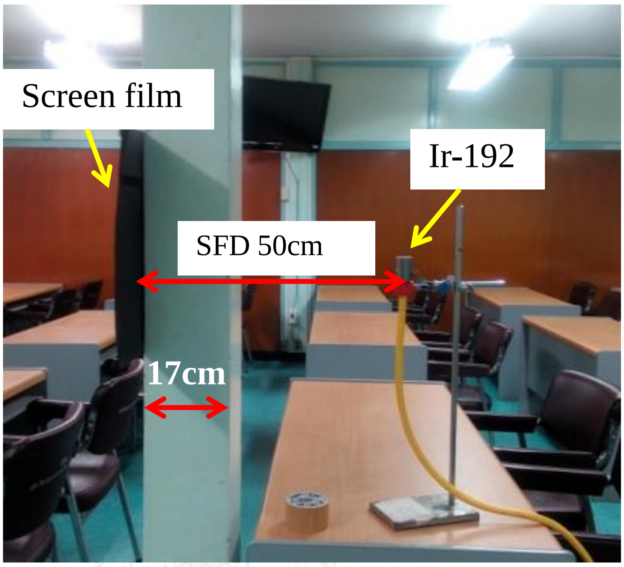

Figure 3.14 Experimental setup of concrete pole radiography

3.3.2 Investigation the real structure of Narayana statue

The Narayana statue made of some kind of rock at Wat Dongsak Tha Maka district in Kanchanaburi province was inspected by the developed technique in comparison to the conventional lead screen-film radiographic technique. The Narayana statue is the remaining antique which was evacuated at Pong Tuk site by the Fine Art Department in 1927 [18]. The evidence indicated that the Narayana statue is cultural art from Dvarawati period around the 11th century. The genuine statue from Dvaravati period was constructed from rock and was supported by frame at both hands and base. However, the appearance of the Narayana state of Wat Dongsak is opaque and is dissimilar from the appearance of the original one due to the renovation. Photos of the Narayana statue of Wat Dongsak and the genuine statue are shown in figure 3.15 (a) and 3.15 (b), respectively. The statue was radiographed by the developed technique using Ir-192 gamma radiation source as in the previous inspection. The experimental setup is shown in figure 3.16

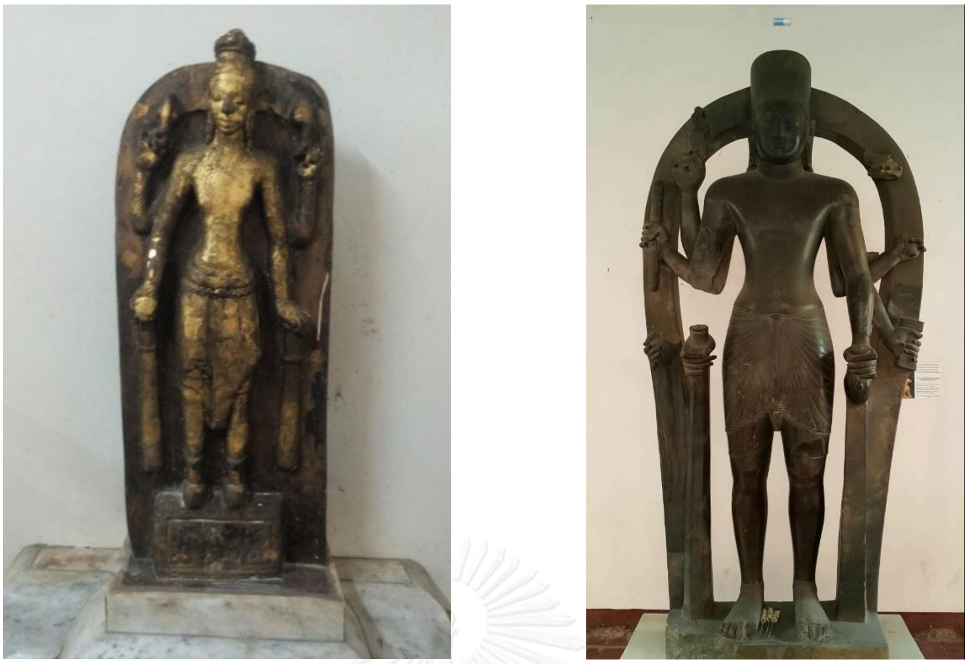

(a) (b)

Figure 3.15 Reconstructed Narayana statue at Wat Dongsak (a) and the original statue in Dvaravati (b)

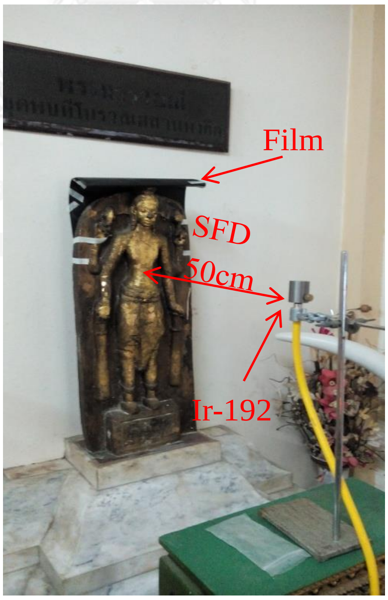

Figure 3.16 Experimental setup for inspection of the Narayana statue by using gamma radiography

3.4 Development of a device for determination of the exposure time by measurement of the transmitted gamma ray intensity

To speed up the film radiography process, not only the technique was developed but also a device for quick determination of the exposure time. The developed device is designed to measure the transmitted gamma intensity after passing through a specimen. The appropriate exposure can then be determined without need of information on specimen thickness and specimen material. Moreover, it is also independent on source activity and source to film distance, which makes radiographic process economical, convenient and more reliable. The gamma-ray detector is essentially small so that the transmitted intensity can be measured at the desired parts of the specimen. This research, therefore, selected a PIN photodiode as the gamma-ray detector which was small and sensitive to x-rays and gamma rays particularly at high dose [19-21]. The device was remotely controlled using an Android mobile phone making the procedure even more convenient and safer [22]. Bluetooth communication allowed up to 10 meters to control the device and to send counting data to the phone. Upon appropriate calibration, the device could also be used to monitor dose rate for safety purpose in industrial radiography and any other radiation practices. The developed device consisted of the following parts.

3.4.1 PIN photodiode

The Si PIN photodiode (Hamamatsu Model s3590-08) having a photo sensitive area of 1 cm^2 was used. The output signal from the PIN photodiode was gained up by a Hamamatsu preamplifier model H4083 which was a charge-sensitive preamplifier with pulse amplifier. The PIN photodiode is shown in figure 3.17

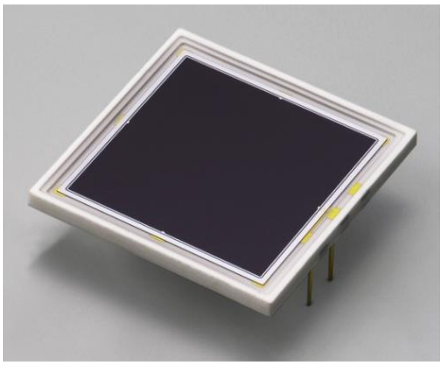

Figure 3.17 Si PIN photodiode [23]

3.4.2 Smartphone

For this research, an Android smartphone was used for data transfer and control of the radiation counting system of the developed device. The Android operating system has been popular and not complicated to develop application software to run on the operating system by using the software development Kit.

3.4.3 Blue tooth module

Recently, almost all smartphones are equipped with Bluetooth module to allow wireless communication between the smartphone and other Bluetooth enabled devices. The range for data communication can be as far as 20 meters or more. In this research, a standard Bluetooth as IEEE 802.15.1 was used as shown in figure 3.18.

Figure 3.18 Bluetooth module

3.4.4 Test specimens for determination of the exposure time using the developed device

The developed device was tested for determination of the exposure time of 3 test specimens including a welded steel plate, a cast iron sample, and a lock shown in figure 3.19

(a)

(b)

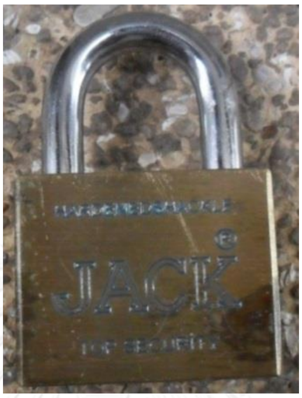

(c)

Figure 3.19 The test specimens for determining the exposure times by the developed device (a) welled steel plate, (b) cast Iron sample and (c) the lock

3.5 Design of the developed device for determination of the exposure time

3.5.1 Radiation counting device using PIN photodiode

The Si Positive-Intrinsic-Negative or PIN photodiode is a semiconductor detector type, which creates electron-hole pairs from interaction of an incident gamma ray with P-N junction. By supplying the reverse-biasing voltage, charges can be then collected [24]. The basic structure of the PIN photodiode is shown in figure 3.20. The PIN photodiode is widely used in the radiation measurement [19-21] due to the above mentioned properties [22] as well as its high-speed response, high sensitivity, low noise and compactness.

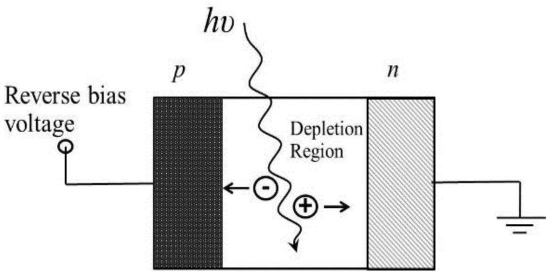

Figure 3.20 Basic structure of PIN photodiode

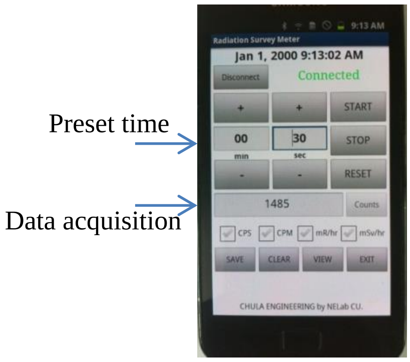

Figure 3.21 Developed user interface run on Android smartphone

The in-house developed radiation counting device is composed of four main parts; a PIN photodiode radiation detector, a pulse shaping circuit, a microcontroller board and a Bluetooth module. The developed counting system can be used for a maximum counting rate of 1×10^5 cps and an exposure rate is up to 300 mR/hr [22]. The android interface software was also developed to control the counting process and data communication as well as to display the counting results.

The software was designed to be simple and user-friendly and its interface is shown in figure 3.21. The pre-set time can be done by touching screen on the menu + and - for increasing and decreasing time, respectively. For the menu START, STOP and RESET, user can remotely controlled to start, to stop and to reset the system via Bluetooth communication. Then the acquisition data will be displayed on the screen. It should be noted that the interface was not only designed for this purpose but also for other applications.

To investigate the relationship between the transmitted gamma-ray intensity and the thickness of specimen, a steel step wedge was used for calibration. The thicknesses of a steel step wedge are 5.48, 6.98, 8.14, 10.72, 11.55, 12.79, 14.30, 16.60, 18.10, 20.00, 21.06, 22.56, 24.00 and 25.33 mm. The PIN photodiode detector Hamamatsu model S3590-08 with an active area of 1 cm × 1 cm was set behind a steel step wedge at 80 cm distance from a 10 Ci Ir-192 radiation source. Small size detector enabled gamma-ray detection at high dose and could be placed at any small inspection area. The obtained signals from the PIN photodiode were counted by the pulse shaping circuit and the results were then delivered to the smartphone. The experimental setup and the schematic diagram of the developed counting device were shown in figure 3.22 (a) and (b), respectively. The relationship between the steel thicknesses and the transmitted counts was carried out.

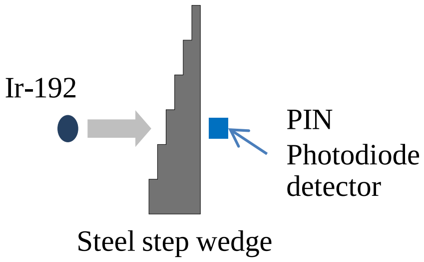

(a)

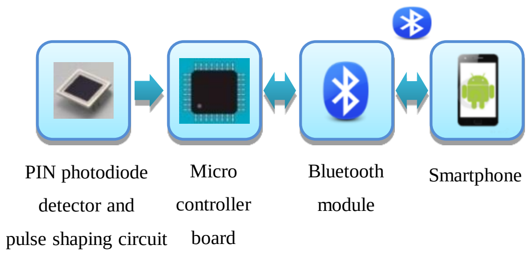

(b)

Figure 3.22 The experimental setup (a) and the schematic diagram of the developed counting device (b)

3.5.2 Film optical density (OD) for various steel thicknesses

For the industrial x-ray and gamma ray radiography with film technique, the film optical density or OD is a conventional factor which indicates image darkness. The OD is defined as the logarithm of inverse of light transmittance. In practice, the OD of the radiographic image should fall in the range of 1 – 3 to keep the image contrast at maximum value [16].

To determine the film OD as a function of the specimen thickness and the exposure time, a steel step wedge was radiographed using Kodak AA 400 x-ray film at exposure times of 5, 10, 15 and 20 minutes, respectively. The experimental setup is shown in figure 3.23. After film processing, the film OD at each steel thickness was measured by a densitometer of Konica model PDA-81. The relationship between the exposure time and the film OD were then plotted for each steel thickness. Subsequently, the film OD calibration chart was created for determination of the appropriated exposure time.

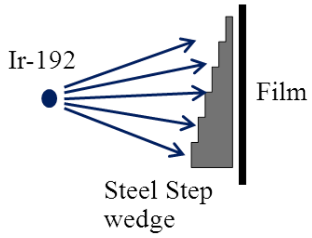

Figure 3.23 Schematic diagram of the experimental setup for determining the film OD at different steel thicknesses

3.5.3 Testing the developed device for determination of exposure time

To test the developed device and method, various types of specimen including a welded steel plate, a cast iron and a lock were radiographed. For the preliminary test, it was aimed to obtain the film OD of 2.0. The developed device was set behind a specimen to measure the transmitted gamma ray intensity. The investigated areas of the samples were indicated in figure 3.24. The obtained counting data were used to determine the appropriated exposure time of each specimen from the calibration chart. The three specimens were finally radiographed using the obtained exposure times. After the film chemical processing, the OD was measured at the position where the transmitted gamma ray intensity was counted to compare with the expected OD of 2.0.

Figure 3.24 Showing the positions on the test specimens where the transmitted gamma-rays were measured with the developed device
(These positions were expected to have the OD of 2.0 on the radiographs)

CHAPTER 4
RESULT AND DISCUSSION

Chapter 4 consists of the 2 sections. The first part contains the results and discussion of factors affecting speed of the screen-film types compared with the conventional lead foil screen-film technique. The following factors were taken into account i.e. the intensifying factor, the image contrast and the image quality which includes resolution, sensitivity and sharpness. Finally, evaluation of the image quality was carried out by using the test specimens in order to compare the developed technique with the conventional film radiography. The second part consists of the results and discussion of the developed technique and device for determining the appropriate exposure times of various test specimens.

4.1 Improvement of radiography speed and investigation of screen-film image quality

4.1.1 Intensifying factors of screen-film types

4.1.1.1 Intensifying factor of metal screens

By increasing the exposure, the film optical densities (OD) was increased. The log relative exposures were plotted with the obtained optical density. Then, the data were fitted with the exponential function as shown in figure 4.1. The intensifying factor of each screen was calculated from antilog of the difference between log relative exposure at OD = 2.0 with and without the intensifying screen. The intensifying factor of dysprosium screen and the lead screen were found to be 1.337 and 1.387, respectively, as shown in table 4.1. The result shows that the intensifying factor of dysprosium screen was not higher than the conventional lead screen as experimented by Bulubay and Tugrul [1] .

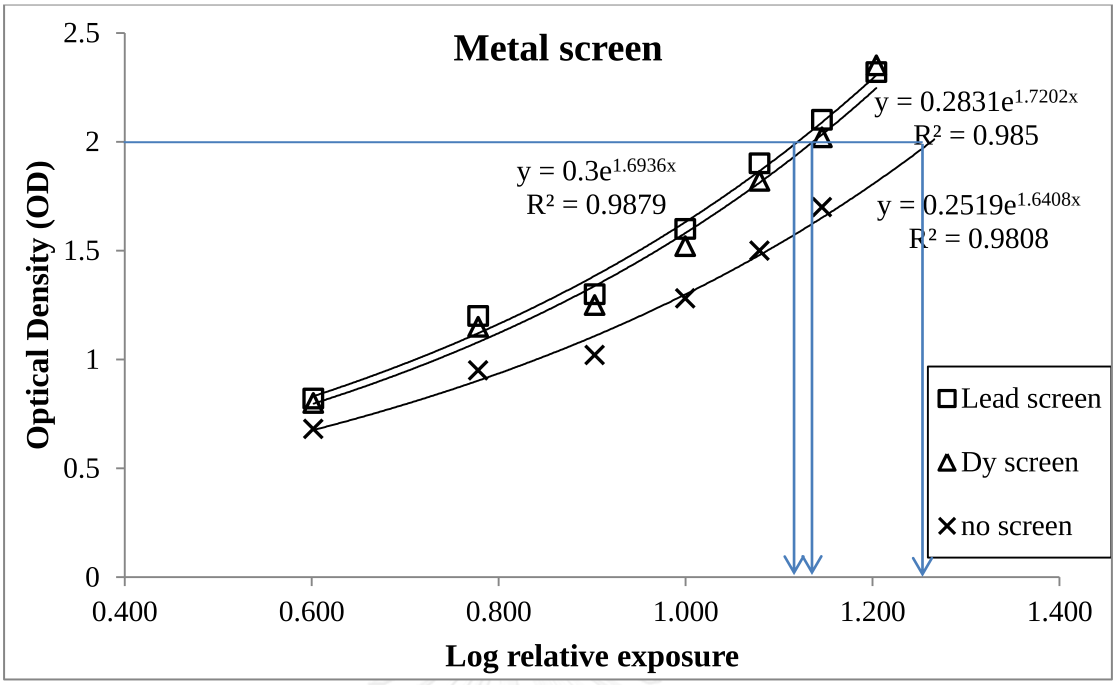

Figure 4.1 Characteristic curve of metal screen-film

Table 4.1 Intensifying factor of metal screen

	Lead screen	Dy screen	No screen
Log relative exposure	1.120	1.136	1.262
Difference*	0.142	0.126	0
Intensifying factor	1.387	1.337	1

* Difference of log relative exposure

4.1.1.2 Intensifying factor of the fluorescent screens

4.1.1.2.1 Intensifying factor of the fluorescent screens with x-ray generator

By varying the exposure at 100, 130 and 160 kVp x-rays, the film OD increased with increase of the exposure time. The obtained data from each kVp were fitted with the exponential function as shown in figure 4.2, 4.3 and 4.4 respectively. The intensifying factor of screen was calculated from the fitted exponential equation at OD = 2.0 as in 4.1.1.1. The intensifying factors were shown in table 4.2, 4.3 and 4.4. It is clearly seen that the PI-200 screen gives the highest speed for x-ray at all energies.

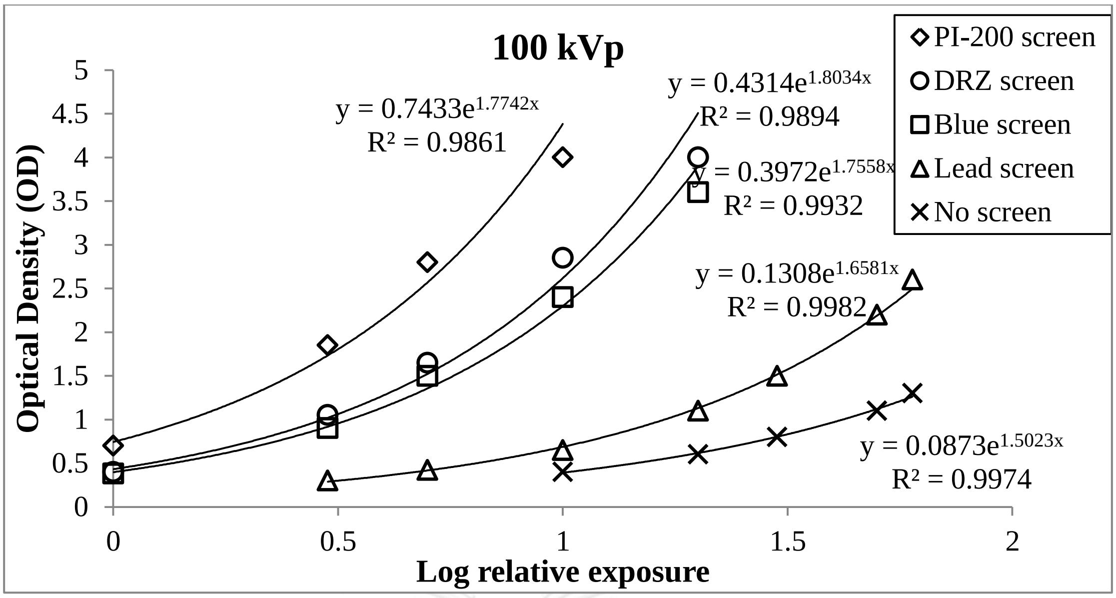

Figure 4.2 Characteristic curve of fluorescent screen-film from 100 kVp x-ray

Table 4.2 Intensifying factor of fluorescent screen from 100 kVp x-ray

	PI-200 screen	DRZ screen	Blue screen	Lead screen	No screen
Log relative exposure	0.557	0.850	0.920	1.644	2.084
Difference*	1.527	1.234	1.164	0.44	0
Intensifying Factor	33.621	17.13	14.583	2.752	1

* Difference of log relative exposure

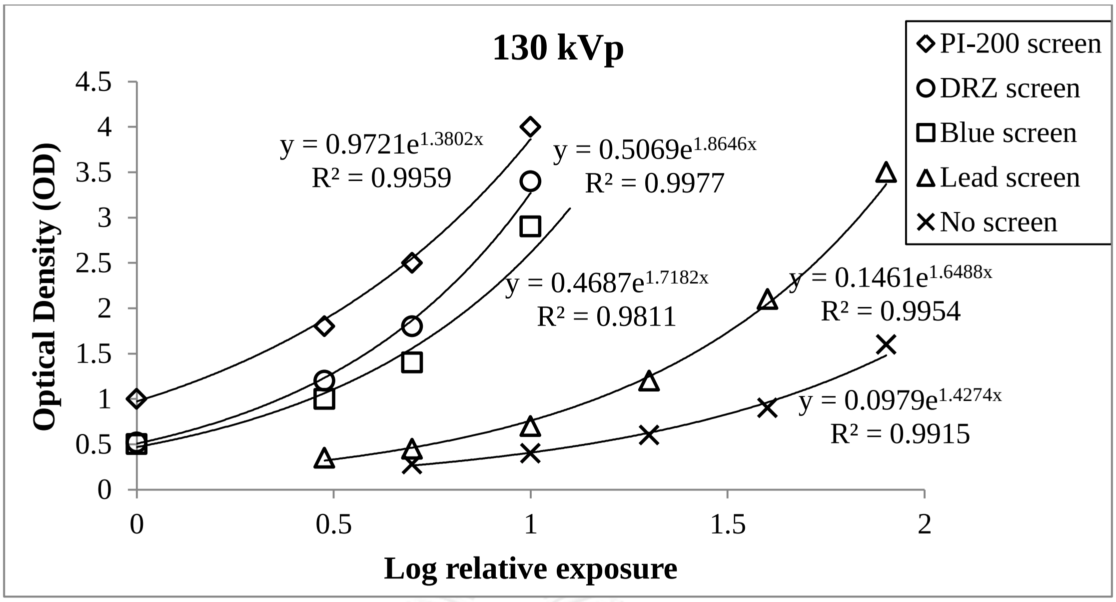

Figure 4.3 Characteristic curve of fluorescent screen-film from 130 kVp x-ray

Table 4.3 Intensifying factor of fluorescent screen from 130 kVp x-ray

	PI-200 screen	DRZ screen	Blue screen	Lead screen	No screen
log relative exposure	0.523	0.736	0.844	1.587	2.114
difference log	1.591	1.377	1.269	0.527	0
Intensifying Factor	38.985	23.849	18.584	3.362	1

* Difference of log relative exposure

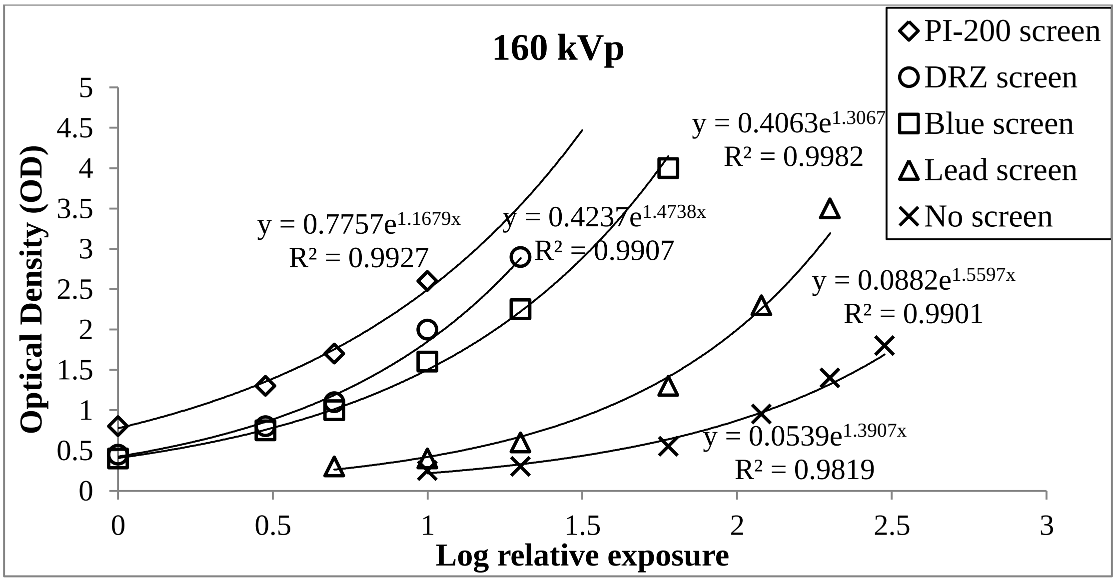

Figure 4.4 Characteristic curve of fluorescent screen-film from 160 kVp x-ray

Table 4.4 Intensifying factor of fluorescent screen from 160 kVp x-ray

	PI-200 screen	DRZ screen	Blue screen	Lead screen	No screen
log relative exposure	0.811	1.053	1.220	2.001	2.599
difference log	1.788	1.546	1.379	0.597	0
Intensifying Factor	61.313	35.120	23.922	3.957	1

* Difference of log relative exposure

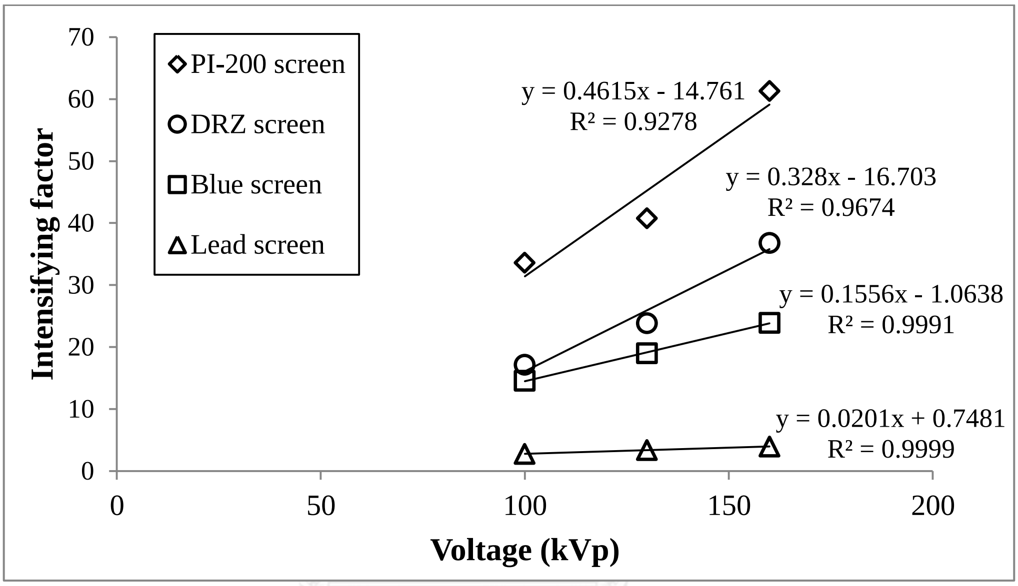

Figure 4.5 Intensifying factor of each screen-film with increasing of the x-ray voltage

Table 4.5 Intensifying factor of each screen-film versus changing of the x-ray voltage

Voltage (kVp)	PI-200 screen	DRZ screen	Blue screen	Lead screen
100	33.621	17.138	14.583	2.752
130	38.985	23.849	18.584	3.362
160	61.313	35.120	23.922	3.957

The results above showed that the intensifying factor increased with increasing the voltage setting of the x-ray generator as show in figure 4.5 and table 4.5. Nevertheless should be kept in mind that the intensifying factor did not increase with increase of x-ray energy. The main reason is that when voltage of x-ray generator increased, the intensity of low energy of x-ray also increased.

4.1.1.2.2 Intensifying factor of fluorescent screen with radioisotope source

For the Ir-192 radiation source, the films were sandwiched by PI-200, the blue screen and the conventional lead screen. For the Co-60 high energy gamma source, the films were sandwiched with the PI-200, DRZ, and the lead screen. The obtained data from each source were fitted with the exponential function as shown in figure 4.6, and 4.7 respectively. The intensifying factor of screen was calculated from the fitted exponential equation at ODs = 2.0 as in 4.1.1.1 The intensifying factors were shown in table 4.6, 4.7. For the comparative evaluation of the result for Ir-192 radiation source as shown in the table 4.6, the intensifying factor of the PI-200 screen was found to be about at 13 times of no screen film and about 7.3, 6.4, and 5.8 times of the PI-200 screen with lead filter, the Blue screen and the conventional lead screen respectively. The intensifying factor of the single screen is approximately half of the double screen. The intensifying factor with Co-60 is shown in table 4.7 which was also consistent with those obtained with Ir-192 and found to about 6 times less than Ir-192.

Relationship between the high energy gamma ray from Co-60 and low energy gamma ray from Ir-192, the result showed that the intensifying factor of Ir-192 is much higher than that of Co-60 for the similar screen-film type. The difference of intensity factor between the Ir-192 and Co-60 for PI-200 screen-film is about 2.3 and about 2.1 for lead screen as shown in figure 4.8 and 4.9. It can be concluded that the intensifying factor decreased with increase in gamma ray energy.

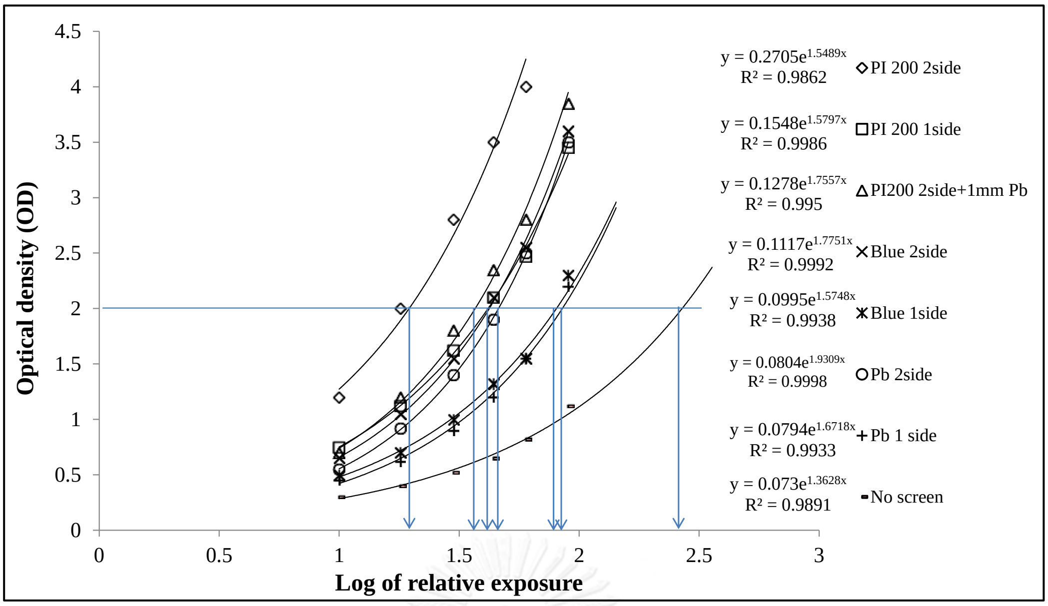

Figure 4.6 Characteristic curve of fluorescent screen-film from Ir-192

Table 4.6 Intensifying factor of fluorescent screen from Ir-192

	PI-200 2side	PI-200 1side	PI-200 2side** +Pb filter	Blue 2side	Blue 1side	Pb 2side	Pb 1 side	No screen
Log relative exposure	1.292	1.620	1.567	1.625	1.905	1.664	1.930	2.429
Difference*	1.138	0.809	0.863	0.804	0.524	0.765	0.499	0
Intensifying Factor	13.725	6.447	7.287	6.364	3.339	5.817	3.157	1

* Difference of log relative exposure

** Film was sandwiched by PI-200 fluorescent screen and with 1 mm lead filter was placed on the top of screen

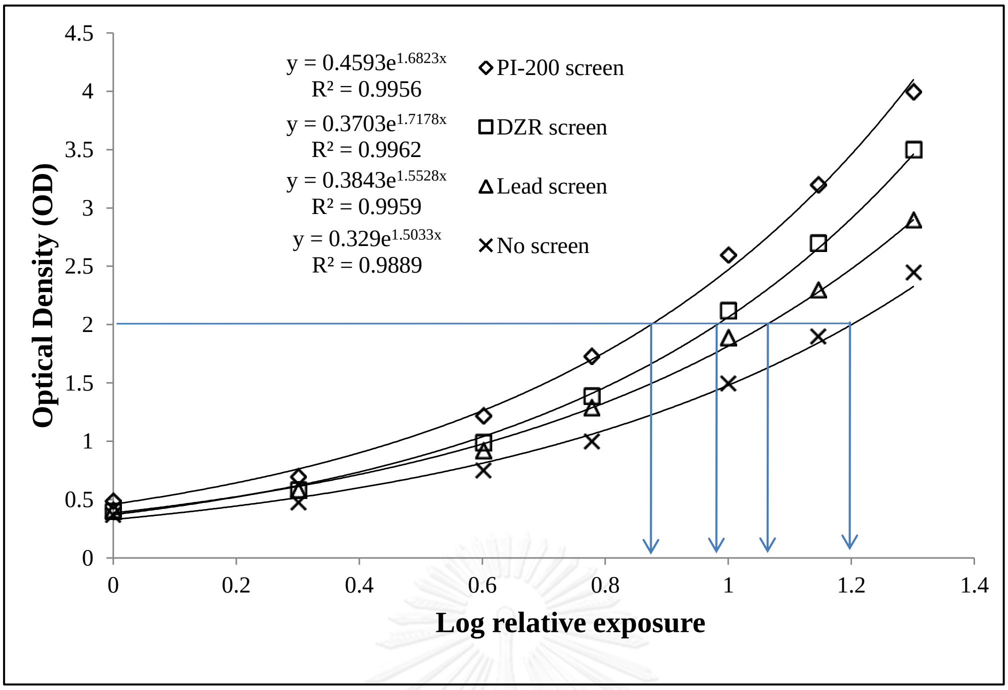

Figure 4.7 Intensifying factor of screen-film with Co-60

Table 4.7 Intensifying factor of fluorescent screen with Co-60 at OD=2.0

	PI-200	DZR	Lead screen	No screen
Log relative exposure	0.830	0.982	1.064	1.201
Difference*	0.371	0.219	0.137	0
Intensifying Factor	2.349	1.655	1.370	1

* Difference of log relative exposure

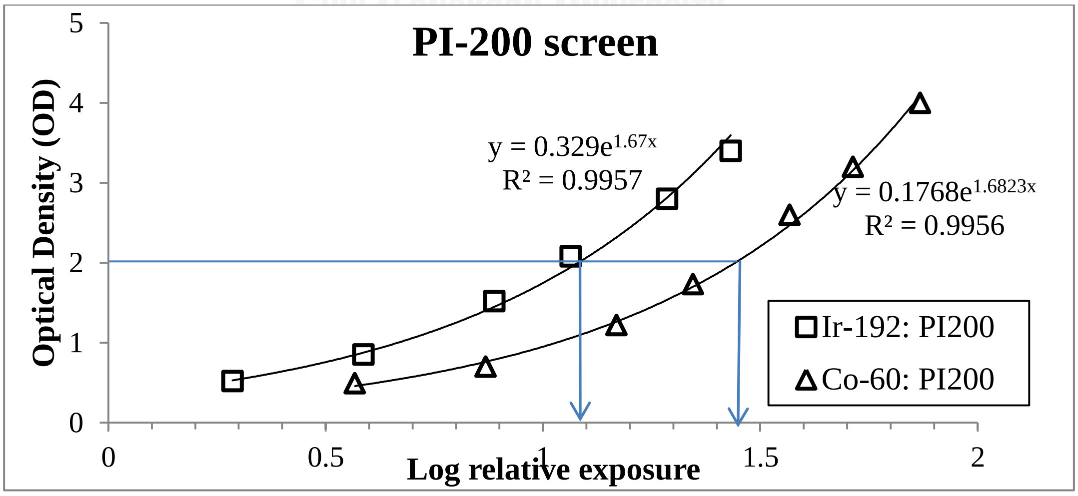

Figure 4.8 Comparison of PI-200 screen intensifying factor from Co-60 high energy gamma and Ir-192 low energy gamma

Table 4.8 Relationship of intensifying factor between Ir-192 and Co-60 for PI-200 screen

	PI-200 screen	
	Ir-192	Co-60
Log relative exposure	1.080	1.442
Difference*	0.362	0
Intensifying Factor	2.297	1

* Difference of log relative exposure

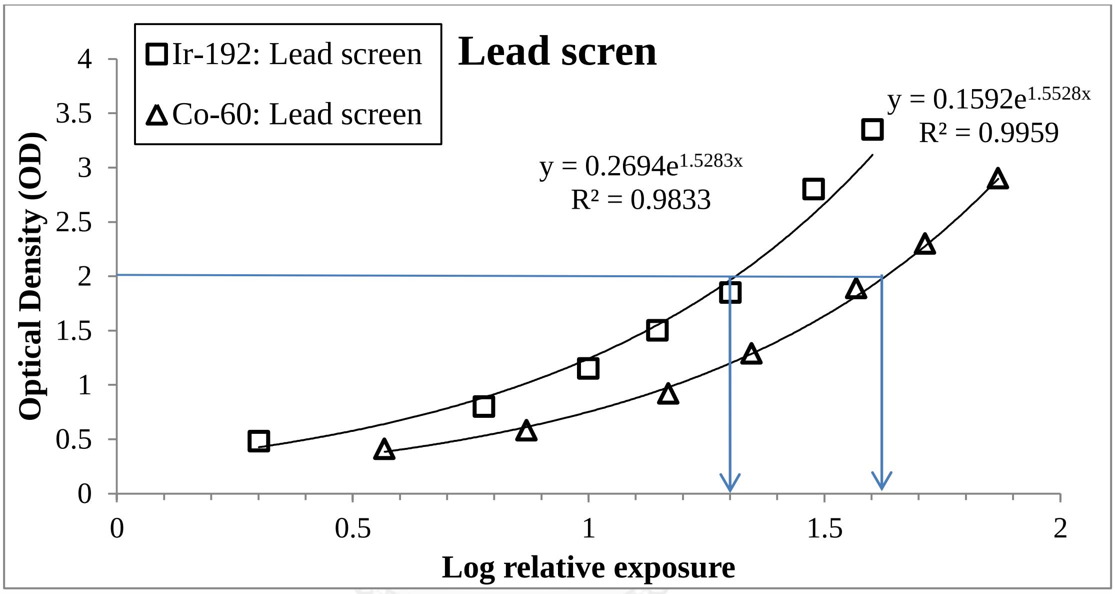

Figure 4.9 Comparison of lead screen intensifying factor from Co-60 high energy gamma and Ir-192 low energy gamma

Table 4.9 Relationship of intensifying factor between Ir-192 and Co-60 for lead screen

	Lead screen	
	Ir-192	Co-60
Log relative exposure	1.311	1.629
Difference*	0.318	0
Intensifying Factor	2.079	1

* Difference of log relative exposure

4.1.2 Investigation of the quality of screen-film radiography

4.1.2.1 Scattered radiation effect testing

For Co-60 source without specimen, the peak to Compton ratio was 0.288. With concrete specimen between the Co-60 source and the detector, the photopeak to Compton ratio decreased with increasing of the concrete thickness as shown in the figure 4.10. By using the peak to Compton ratio of 0.288 for the detector, the net Compton intensity at each concrete thickness can be obtained from

Intensity of Compton continuum – 0.288 x intensity of photopeak,

which is tabulated in Table 4.10 and showed graphically in figure 4.11. It could be noticed that the net Compton intensity increased with increase of concrete thickness up to 8 cm then level off.

Table 4.10 Gamma scatter with increasing concrete thickness

Thickness of Concrete (cm)	Compton Scattering (Counts/300sec)	Photopeak (Counts/300sec)	Peak to Compton Ratio	Gamma scattered from concrete (Counts/300sec)
0	188097	654078	0.288	0
2	149585	608373	0.246	88215
4	114181	558881	0.204	161834
6	89074	502172	0.177	192431
8	70601	446203	0.158	200699
10	55216	383349	0.144	191344
12	43728	331105	0.132	179048
14	34297	280837	0.122	161575
16	26672	236422	0.113	143674
18	20640	198432	0.104	126660
20	16231	167628	0.097	111187

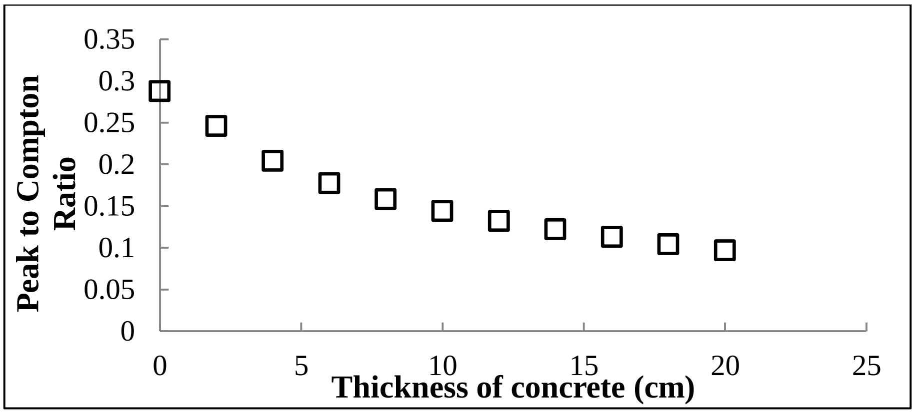

Figure 4.10 Relationships between peak to Compton Ratio and thickness of concrete

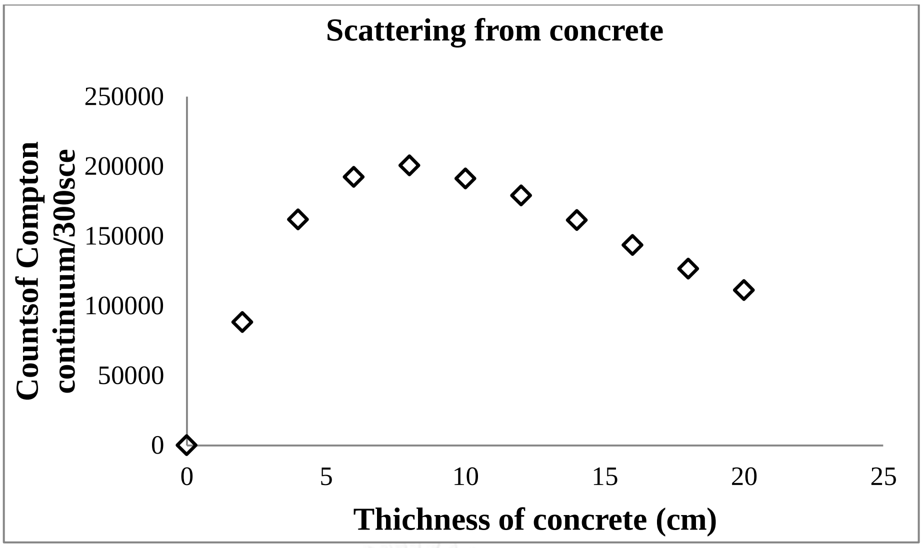

Figure 4.11 Intensity of Compton continuum versus concrete thickness

4.1.2.2 Reduction of scattered gamma ray using lead filter

To reduce the scatted gamma rays from concrete, the lead sheet filter was inserted between the screen and the specimens. The obtained data was described the peak to Compton ratio increased with increasing the lead sheet filter which inserts between the detector and the 8 cm of concrete specimens, it might be presumed that the lead sheet filter can be reduced the scatted gamma ray from concrete 8 cm as shown in figure 4.13 whereas, increasing the lead filter more than 3 mm might be reduce the peak to Compton ratio. Therefore, the 1 mm of lead thickness was sufficient to filter the scattered from specimens.

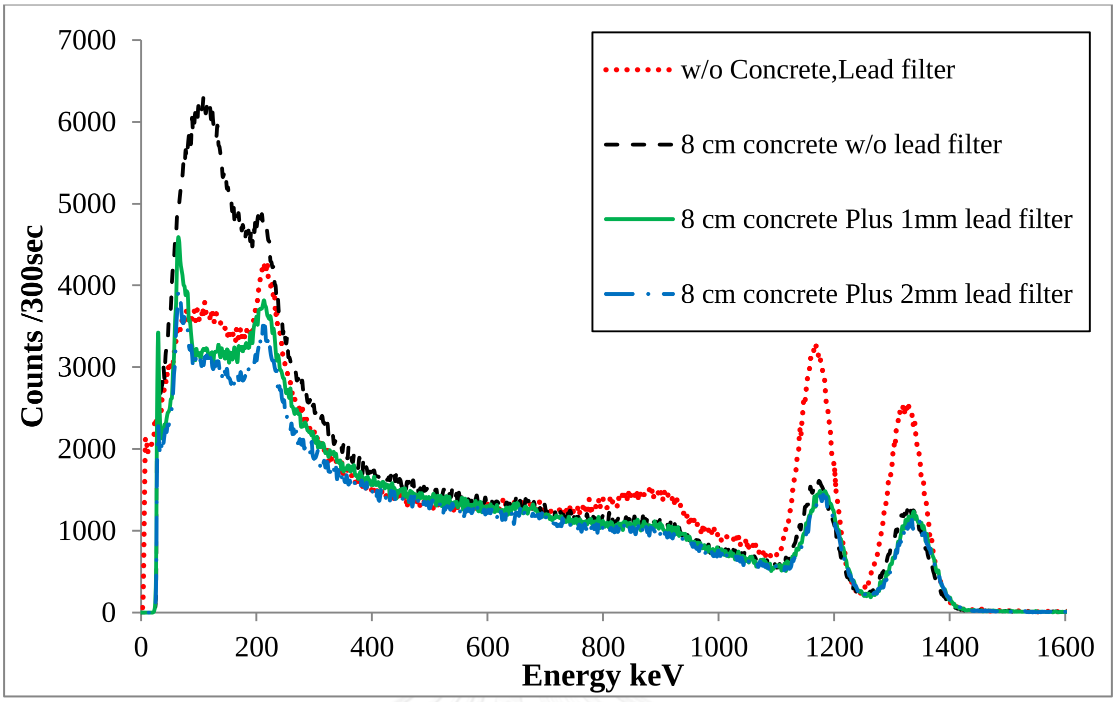

Figure 4.12 Spectrum of Co-60 gamma ray which penetrate through to 8 cm concrete with and without lead filter

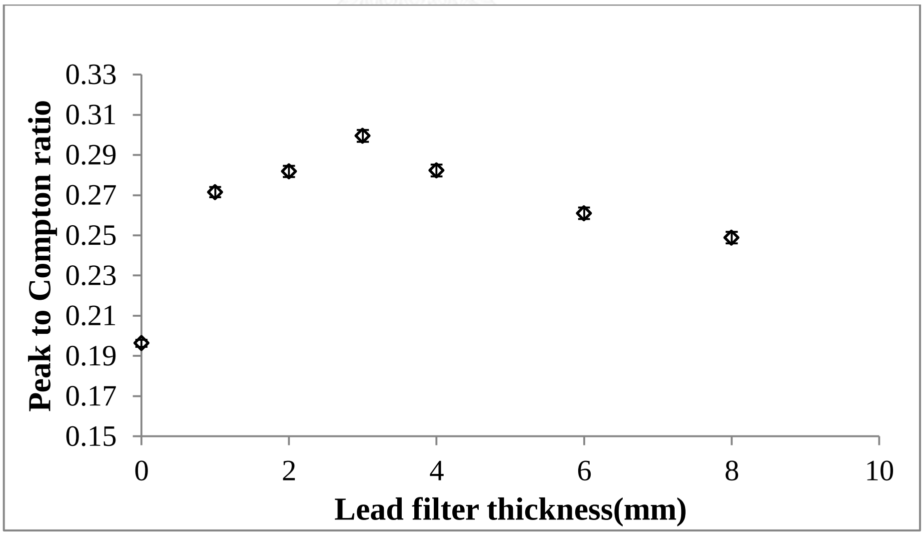

Figure 4.13 Relationships between peak to Compton ratio and thickness of lead sheet filter

4.1.2.3 Radiographic contrast of screen-film radiography

4.1.2.3.1 Radiographic contrast of screen-film radiography using x-ray generator

The radiographic contrast composes of material contrast and film contrast. The film gradient or film contrast is the slope of the characteristic cure of screen-film, the straight line of characteristic curve, optical density range 1.5-3 was used for this experiment. By varying the exposure, the OD increased with increasing the exposure time which the obtained data of each screen-film were fitted with linear function of OD and log relative exposure as shown in figure 4.14, 4.15 and 4.16 with vary voltage of x-ray generator were 100 kVp, 130 kVp and 160 kVp, respectively. From the result, film screen contrast of each screen as shown in table 4.11, 4.12 and 4.13 of 100 kVp, 130 kVp and 160 kVp respectively that the screen-film contrast or slope of liner function quite approximate for the increasing x-ray voltage which film with screen, PI-200 screen, DRZ screen, Blue screen and lead screen were similar trend except the no screen slope less than group of screen-film.

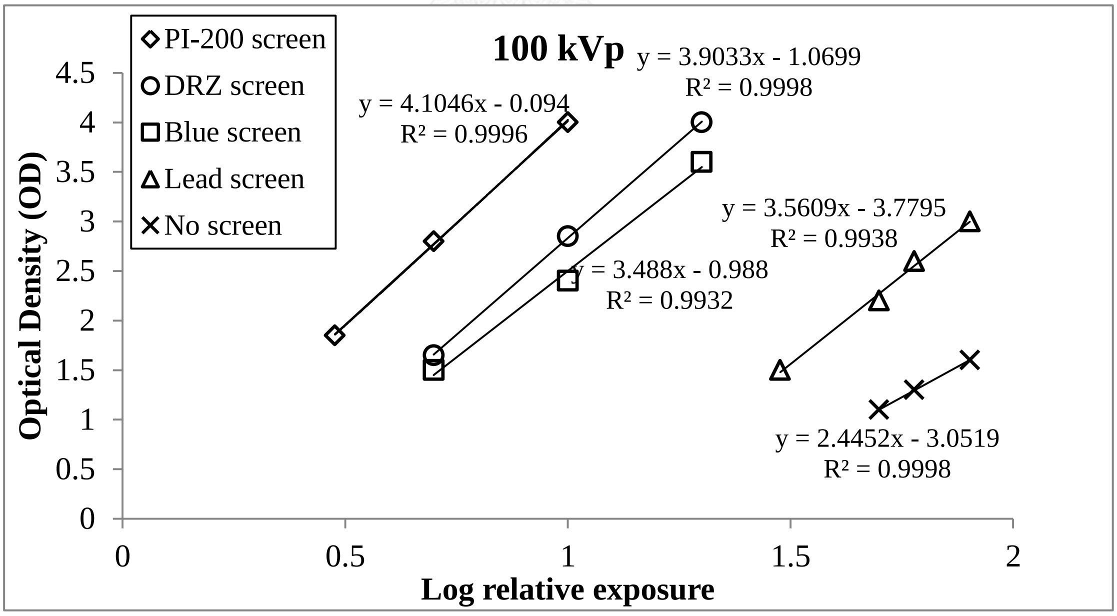

Figure 4.14 Straight line portion of characteristic curve of fluorescent screen-film from 100 kVp x-ray

Table 4.11Contrast of screen-film with 100 kVp x-ray generator

Type of screen	contrast
PI-200 screen	4.104
DRZ screen	3.903
Blue screen	3.488
Lead screen	3.560
No screen	2.445

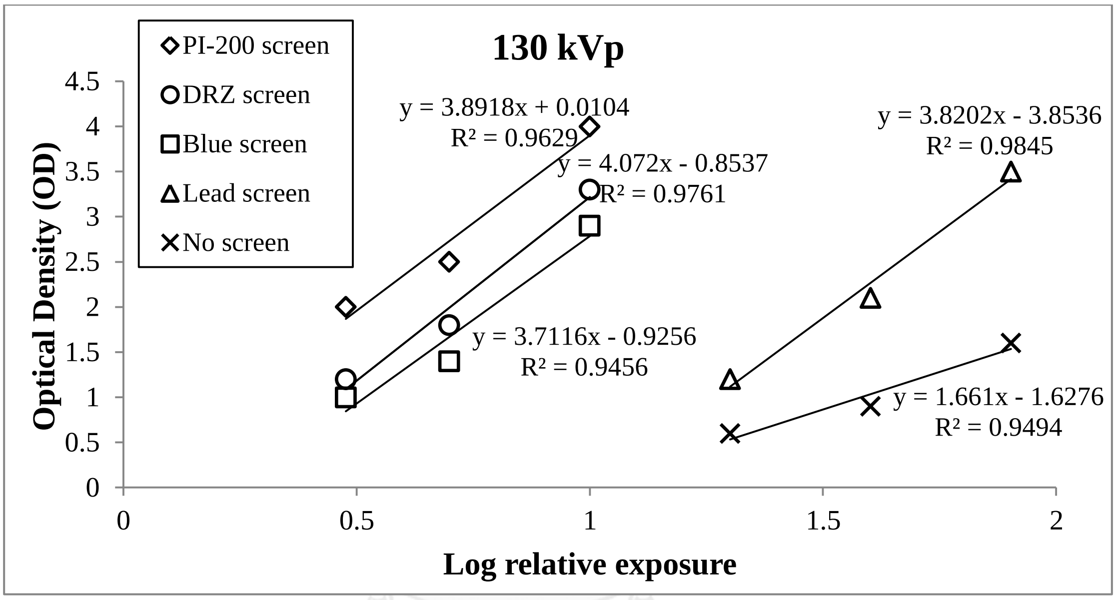

Figure 4.15 Straight line portion of characteristic curve of fluorescent screen-film from 130 kVp x-ray

Table 4.12 Contrast of screen-film with 130 kVp x-ray generator

Type of screen	contrast
PI-200 screen	3.891
DRZ screen	4.072
Blue 2 screen	3.711
Lead 2 screen	3.820
no screen	1.661

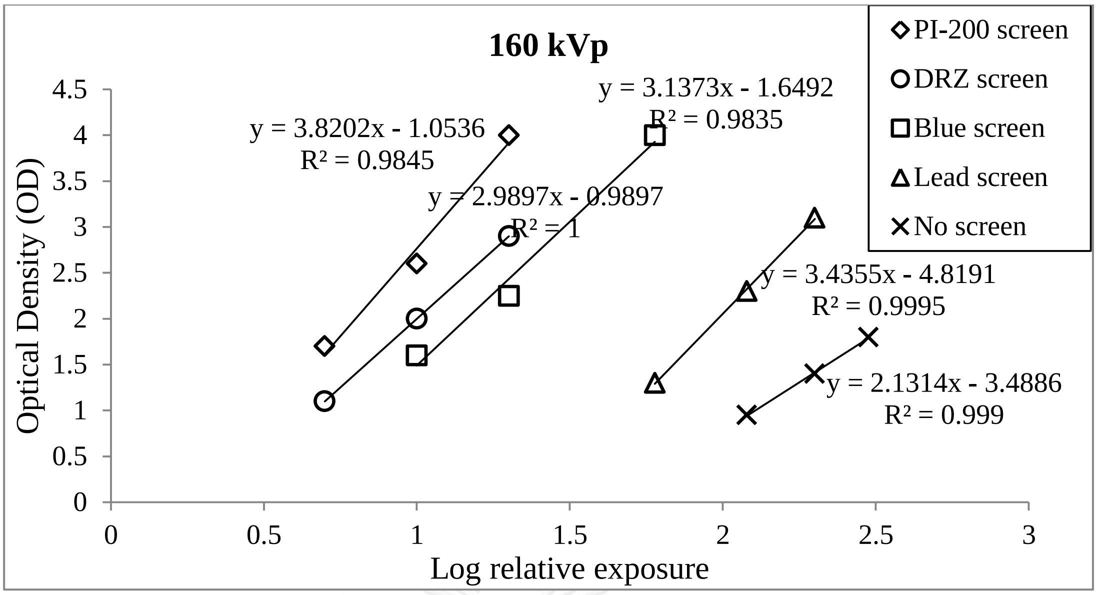

Figure 4.16 Straight line portion of characteristic curve of fluorescent screen-film from 160 kVp x-ray

Table 4.13 Contrast of screen-film with 160 kVp x-ray generator

Type of screen	contrast
PI-200 screen	3.820
DRZ screen	2.989
Blue 2 screen	3.137
Lead 2 screen	3.425
no screen	2.131

4.1.2.3.2 Radiographic contrast of screen-film radiographed with radioisotope source

In figure 4.17 and table 4.14, for the low energy of Ir-192 gamma ray source, the result of screen-film contrast quite similar with the x-ray generator source. On the other hand, for the high gamma ray energy of Co-60 found that the contrast or slope of the screen-film was approximately similar with the contrast of no screen as shown in figure 4.18 and the contrast value of each screen-film in table 4.15.

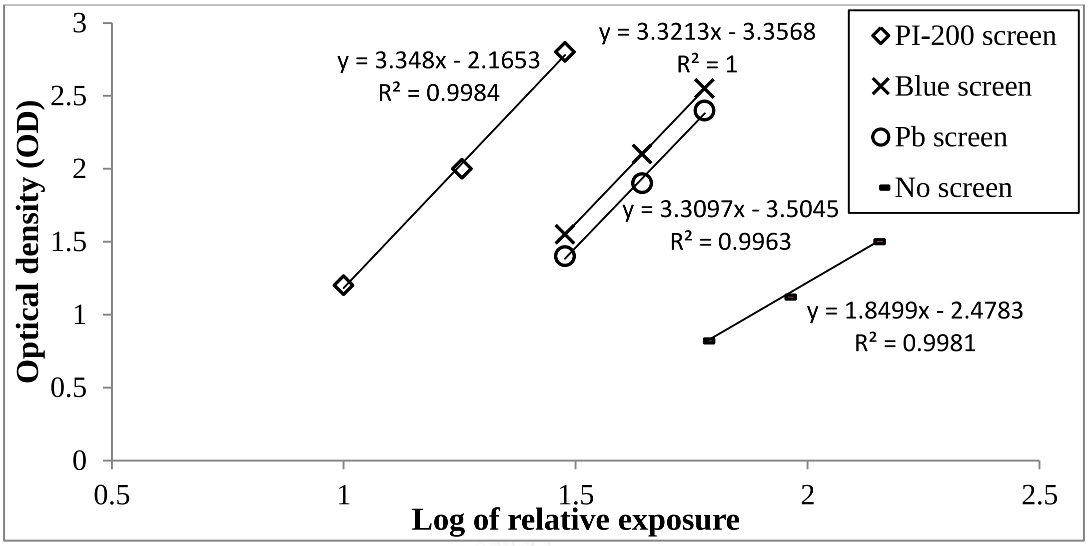

Figure 4.17 Straight line portion of characteristic curve of fluorescent screen-film from Ir-192 radioisotope source

Table 4.14Contrast of screen-film with using Ir-192 radiation source

Screen type	contrast
PI-200 screen	3.348
Blue screen	3.321
Lead screen	3.309
No screen	1.849

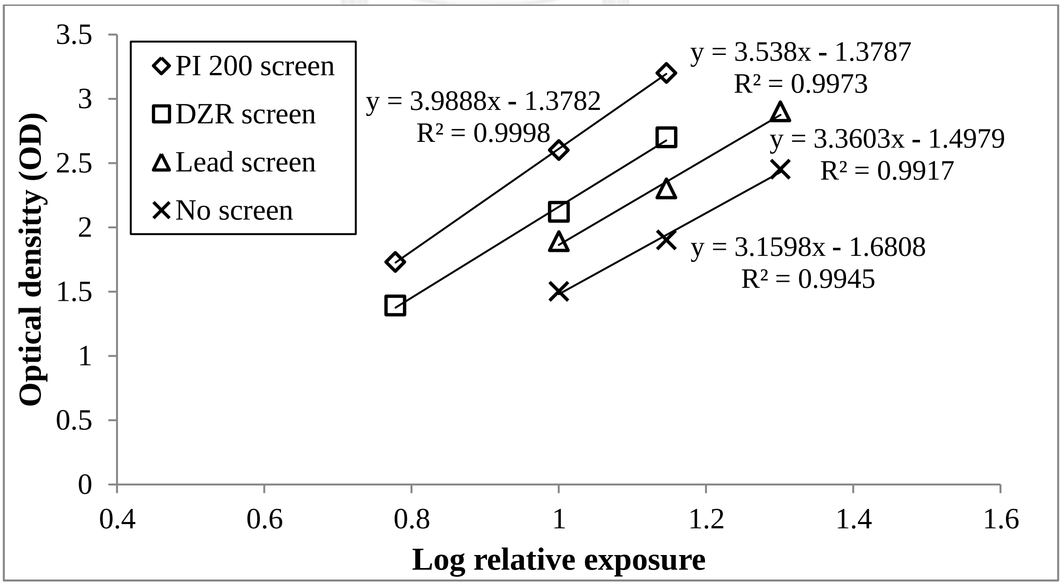

Figure 4.18 Straight line portion of characteristic curve of fluorescent screen-film from Co-60 radioisotope source

Table 4.15 Contrast of screen-film with using Co-60 radiation source

Screen type	contrast
PI-200 screen	3.988
DRZ screen	3.538
Lead screen	3.360
No screen	3.159

4.1.2.4 Sensitivity of radiograph

4.1.2.4.1 Sensitivity of the screen-film radiography using x-ray generator

For non-destructive testing in industrial for radiographic technique that the image quality can be determined from the sensitivity, which is measured by indicator for this experiment we used the wire type of Image Quality Indicator (IQI), diameter from DIN IQI 1 FE and DIN IQI 6 FE, place on the 1.5 cm thickness of steel. The sensitivity can be calculated from the diameter smallest wire visible on the radiograph, which being calculated as wire diameter divides by the thickness of steel as equation (2.23). Furthermore, the smallest wire was determined by profile of gray value and distance pixels which relate with the position of wire IQIs in the part of x-ray source as show in figure 4.19. 4.20 and 4.21 for film with lead screen varying voltage of x-ray at 100,130 and 160 kVp , in figure 4.22, 4.23 and 4.24 for film with blue screen varying voltage of x-ray at 100, 130 and 160 kVp, in figure 4.25, 4.26 and 4.27 for film with PI-200 screen varying voltage of x-ray at 100, 130 and 160 kVp, respectively.

The result showed that increase in voltage of the x-ray generator would have little effect on the sensitivity of screen-film, inversely type of screen clearly affected the sensitivity. It was found that the sensitivity of PI-200 screen-film was larger than those of the blue screen and the lead screen. That was most probably because the PI200 screen was thicker than other screens resulted in greater lateral spread of light.

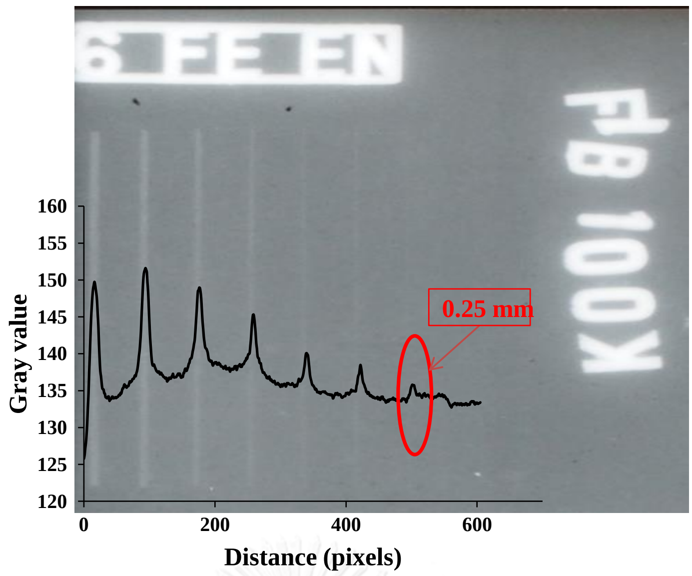

Figure 4.19 Profile of gray level across the wire type IQIs on the radiograph using the convetional lead screen-film technique taken with 100 kVp of x-rays

% sensitivity of film with lead screen at 100 kVp of x-ray = (0.25/15)×100 = 1.67%

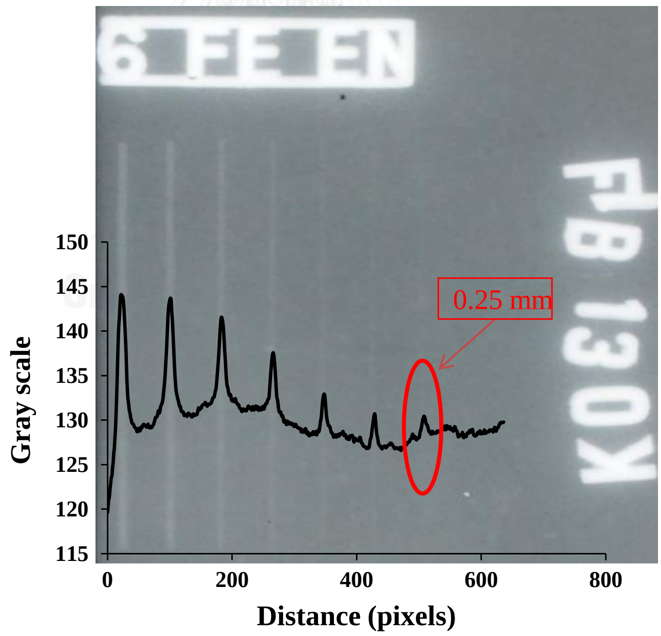

Figure 4.20 Profile of gray level across the wire type IQIs on the radiograph using the convetional lead screen-film technique taken with 130 kVp of x-rays

% sensitivity of film with lead screen at 130 kVp of x-ray = (0.25/15)×100 = 1.67%

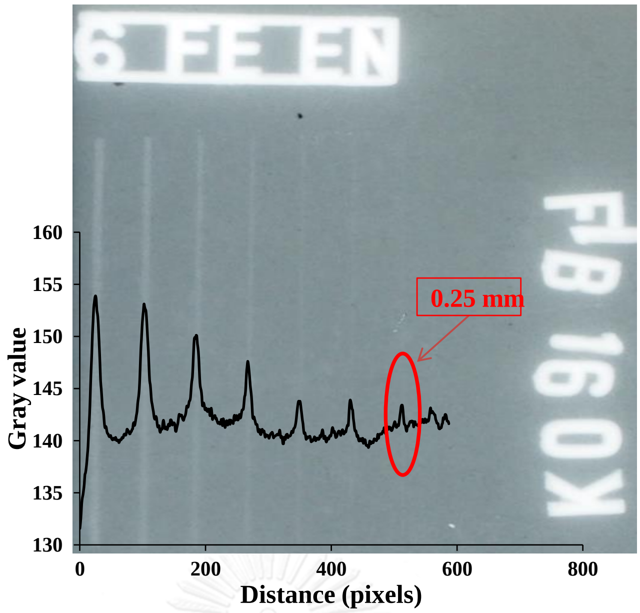

Figure 4.21 Profile of gray level across the wire type IQIs on the radiograph using the convetional lead screen-film technique taken with 160 kVp of x-rays

% sensitivity of film with lead screen at 160 kVp of x-ray = (0.25/15)×100 = 1.67%

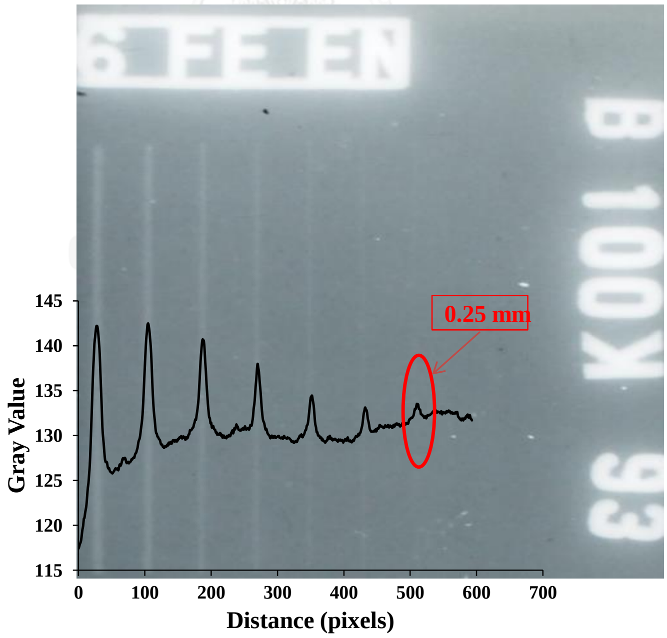

Figure 4.22 Profile of gray level across the wire type IQIs on the radiograph using the Blue screen film technique taken with 100 kVp of x-rays

% sensitivity of film with Blue screen at 100 kVp of x-ray = (0.25/15)×100 = 1.67%

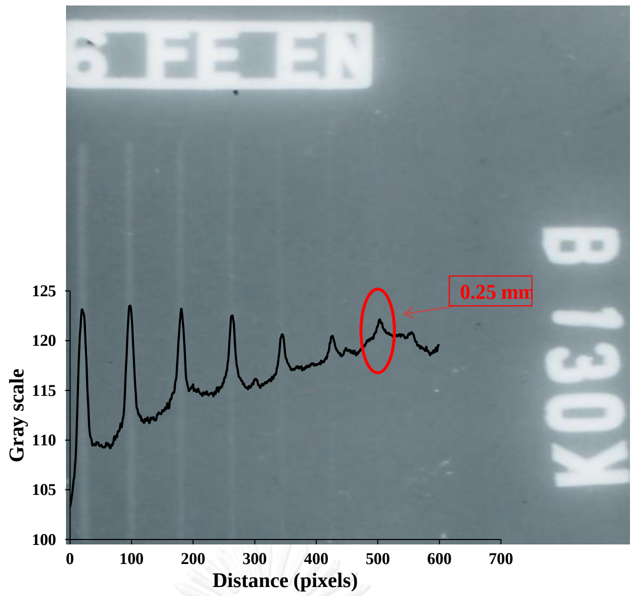

Figure 4.23 Profile of gray level across the wire type IQIs on the radiograph using the Blue screen film technique taken with 130 kVp of x-rays

% sensitivity of film with Blue screen at 130 kVp of x-ray = (0.25/15)×100 = 1.67%

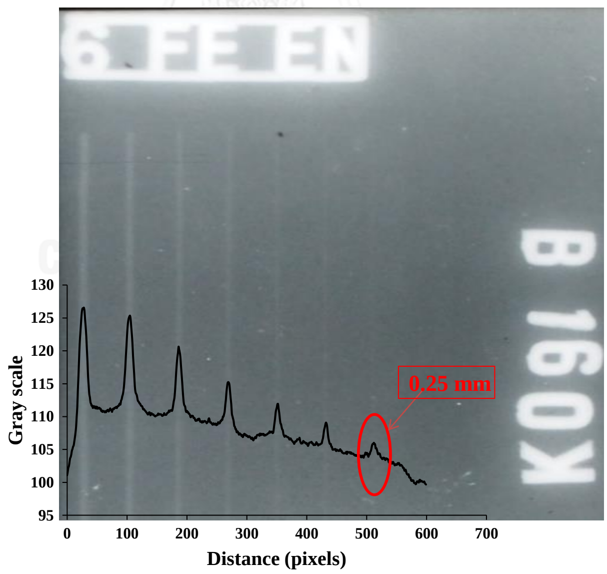

Figure 4.24 Profile of gray level across the wire type IQIs on the radiograph using the Blue screen film technique taken with 160 kVp of x-rays

% sensitivity of film with Blue screen at 160 kVp of x-ray = (0.25/15)×100 = 1.67%

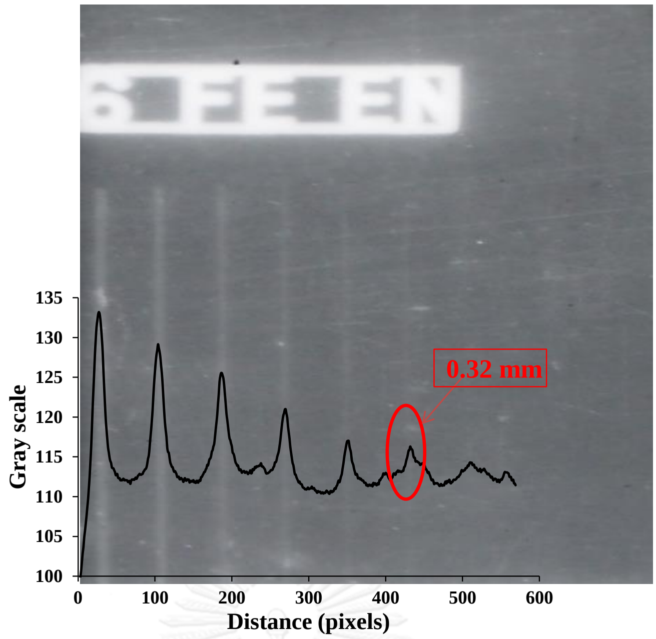

Figure 4.25 Profile of gray level across the wire type IQIs on the radiograph using the PI-200 screen-film technique taken with 100 kVp of x-rays

% sensitivity of film with PI-200 screen at 100 kVp of x-ray = (0.32/15)×100 = 2.13%

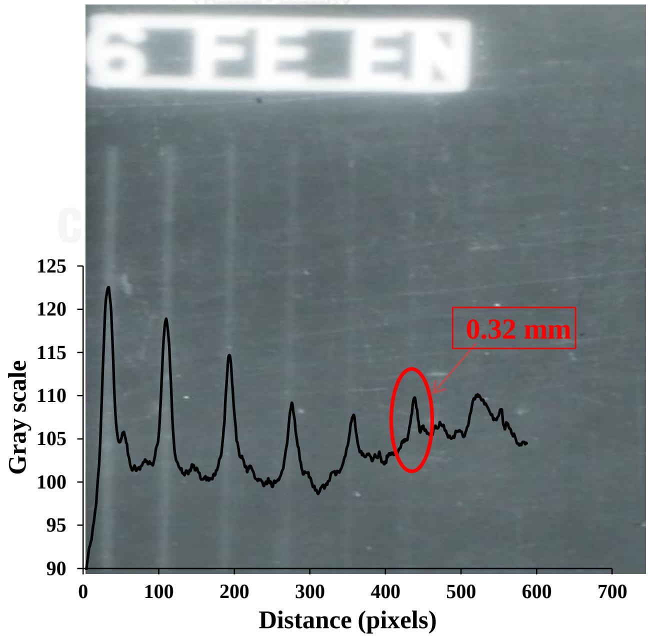

Figure 4.26 Profile of gray level across the wire type IQIs on the radiograph using the PI-200 screen-film technique taken with 130 kVp of x-rays

% sensitivity of film with PI-200 screen at 130 kVp of x-ray = (0.32/15)×100 = 2.13%

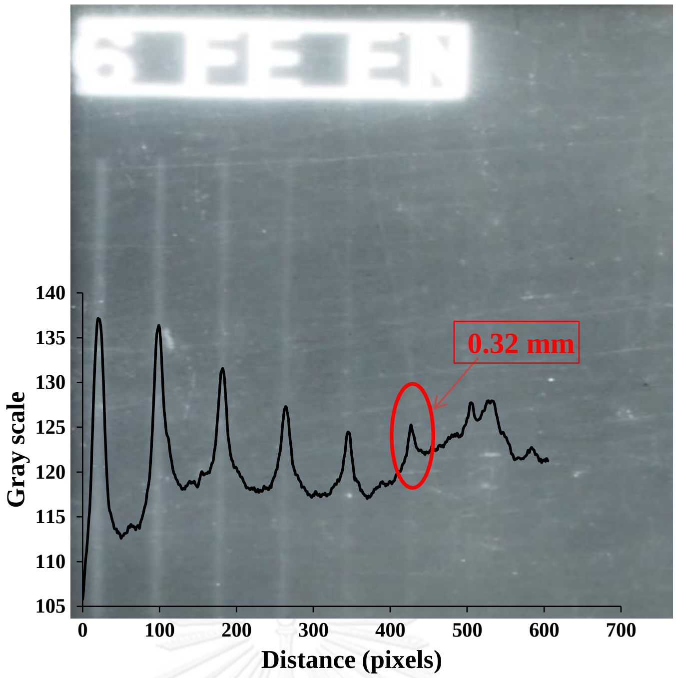

Figure 4.27 Profile of gray level across the wire type IQIs on the radiograph using the PI-200 screen-film technique taken with 160 kVp of x-rays

% sensitivity of film with PI-200 screen at 160 kVp of x-ray = (0.32/15)×100 = 2.13%

Table 4.16 Sensitivity of each screen-film was exposured x-ray generator

% sensitivity of screen-film			
Type of screen	X-ray Voltage		
	100 kVp	130 kVp	160 kVp
PI-200 screen	2.13%	2.13%	2.13%
Blue screen	1.67%	1.67%	1.67%
Lead screen	1.67%	1.67%	1.67%

4.1.2.4.2 Sensitivity of the screen-film radiography using radioisotope source

To determine the sensitivity, the wire type of Image Quality Indicator (IQI), DIN IQI 1FE diameter from DIN IQI 1 FE and DIN IQI 6 FE was used to indication which place in front of the specimens was radiographed by Ir-192 gamma radiation source. For this experiment was used 2 type of specimen are the 2 cm thickness of steel and the 15 cm from concrete block with the 2 cm diameter steel rod inside. The sensitivity can be calculated from the diameter smallest wire visible on the radiograph, which being calculated as wire diameter divides by the thickness of steel as equation 2.23. Furthermore, the smallest wire was determined by profile of gray value and distance pixels which relate with the position of wire IQIs as show in figure 4.29. 4.30, 4.31and 4.32 for film with lead screen, blue screen, PI-200 screen and, PI-200 screen plus 1mm lead sheet, respectively for the 2 cm steel place specimens and figure 4.33 for the another specimens.

The result found that sensitivity was depended on type of screen, the % sensitivity of PI-200 screen is 2.5% which was found to be apparently higher than another screen at 2%. Therefore, the lead sheet filter should be also taken into consideration to reduce the %sensitivity. For experiment the 1 mm lead sheet thickness was filtered the scattered gamma to achieve the reducing of %sensitivity equal 2% in table 4.18.

For the concrete block specimens, the result show that the PI-200 screen plus the lead filter was gained the image quality. Whereas, increased thickness of the lead sheet filter to 2 mm and 3 mm that the result was found to be little effect of reducing sensitivity as shown in figure 4.33.

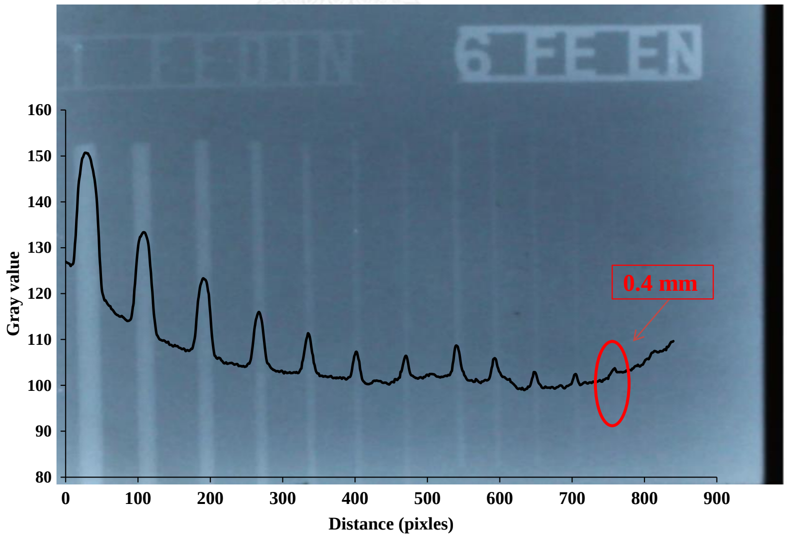

Figure 4.28 Profile of gray value compare with wire type IQIs of film with lead screen was exposured Ir-192 radiation source

% sensitivity of film with Lead screen from Ir-192 = (0.4/20)×100 = 2%

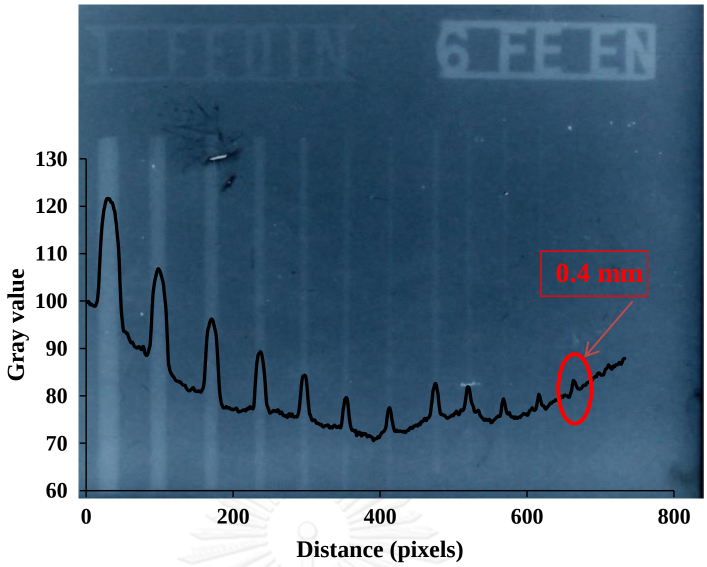

Figure 4.29 Profile of gray value compare with wire type IQIs of film with Blue screen was exposured Ir-192 radiation source

% sensitivity of film with Blue screen from Ir-192 = (0.4/20)×100 = 2%

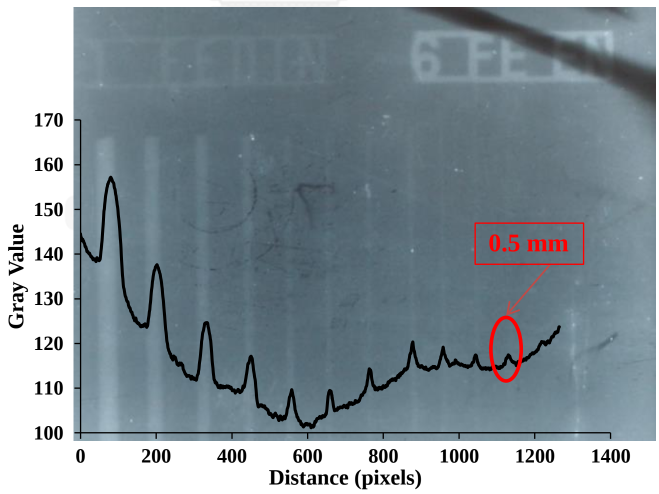

Figure 4.30 Profile of gray value compare with IQI wire of film with PI-200 screen was exposured Ir-192 radiation source

% sensitivity of film with PI-200 screen from Ir-192 = (0. 5/20)×100 = 2.5%

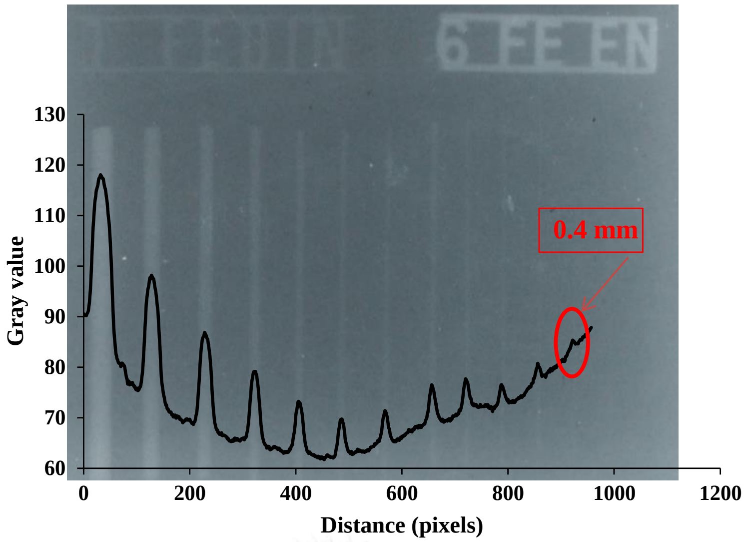

Figure 4.31 Profile of gray level across the wire type IQIs on the radiograph using the PI-200 screen-film technique with 1mm lead filter taken with Ir-192 source

% sensitivity of film with PI-200 screen plus1mm Lead filter from Ir-192
= (0.4/20)×100 = 2%

Table 4.17 Sensitivity of screen-film was exposured Ir-192 radiation source

Type of screen	%sensitivity
lead screen	2
Blue screen	2
PI-200 screen	2.5
PI-200 screen plus 1mm lead filter	2

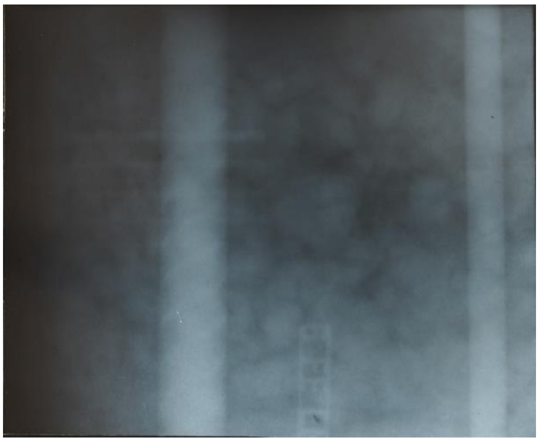

(a)

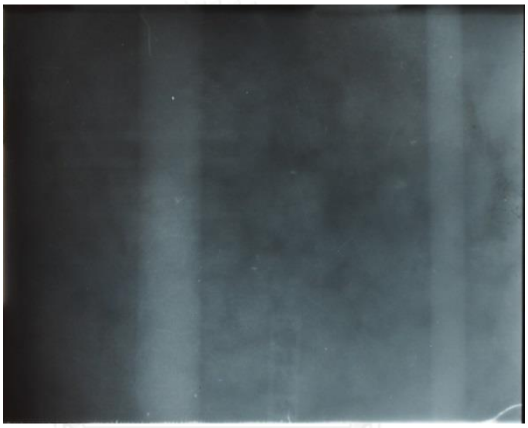

(b)

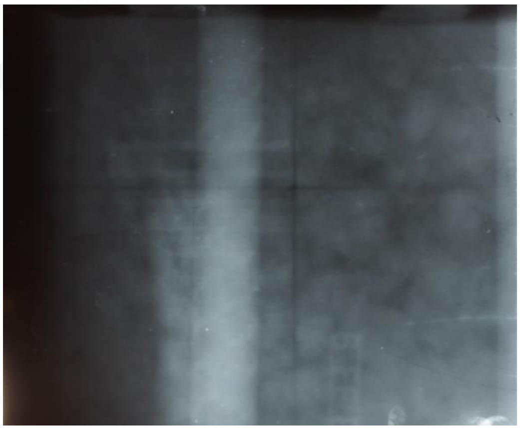

(c)

Figure 4.32 Radiograph of the steel bars within the concrete block including wire type IQIs taken by film with lead screen (a), with PI-200 screen (b) and with PI-200 and 1mm lead filter (c)

4.2 Testing of the developed technique with thick specimens containing light elements

4.2.1 Investigation a concrete pole structure

The figure 4.33 demonstrated that radiographc image of steel bar structure inside the pole of nuclear engineering department, Chulalongkorn University, building which radiographic image with lead screen, PI-200 screen and PI-200 screen with lead filter as shown in figure 4.33 (a), 4.33 (b) and 4.33 (c), respectively. The exposure time of lead screen, PI-200 screen and PI-200 screen with 1 mm lead filter were 70, 30, and 55 minutes respectively. The radiographic images using lead screen and PI200 screen with 1mm lead flter were comaparable and were clear enough to see the detail of steel bars, foreign matter, void and corrosion of concrete as shown in figures 4.33 (a) and 4.33 (c) but the PI200 with lead filter required only 78% of the exposure time for the convetional lead screen-film technique.

4.2.2 Inspection of the Narayana statue

The Narayana statue is still open for discussion to discover the original of architectural style. For this research the original structure of Narayana statue was investigated by screen-film radiographic technique by using Ir-192 gamma source. The figure 4.34 was shown the image of structure of Narayana statue radiographed with the lead screen film for 30 minute of exposure time and the figure 4.35 was shown the image of structure of Narayana statue radiographed with the PI-200 screen film for 12 minute of exposure time. The both image, were revealed the clearly evidence of original structure of Narayana statue which the original structure might have some relation to the architectural style from Dvaravati. However, it can be concluded that PI-200 screen film can be reduce the exposure time for radiography, while the image keep in quality of the detail.

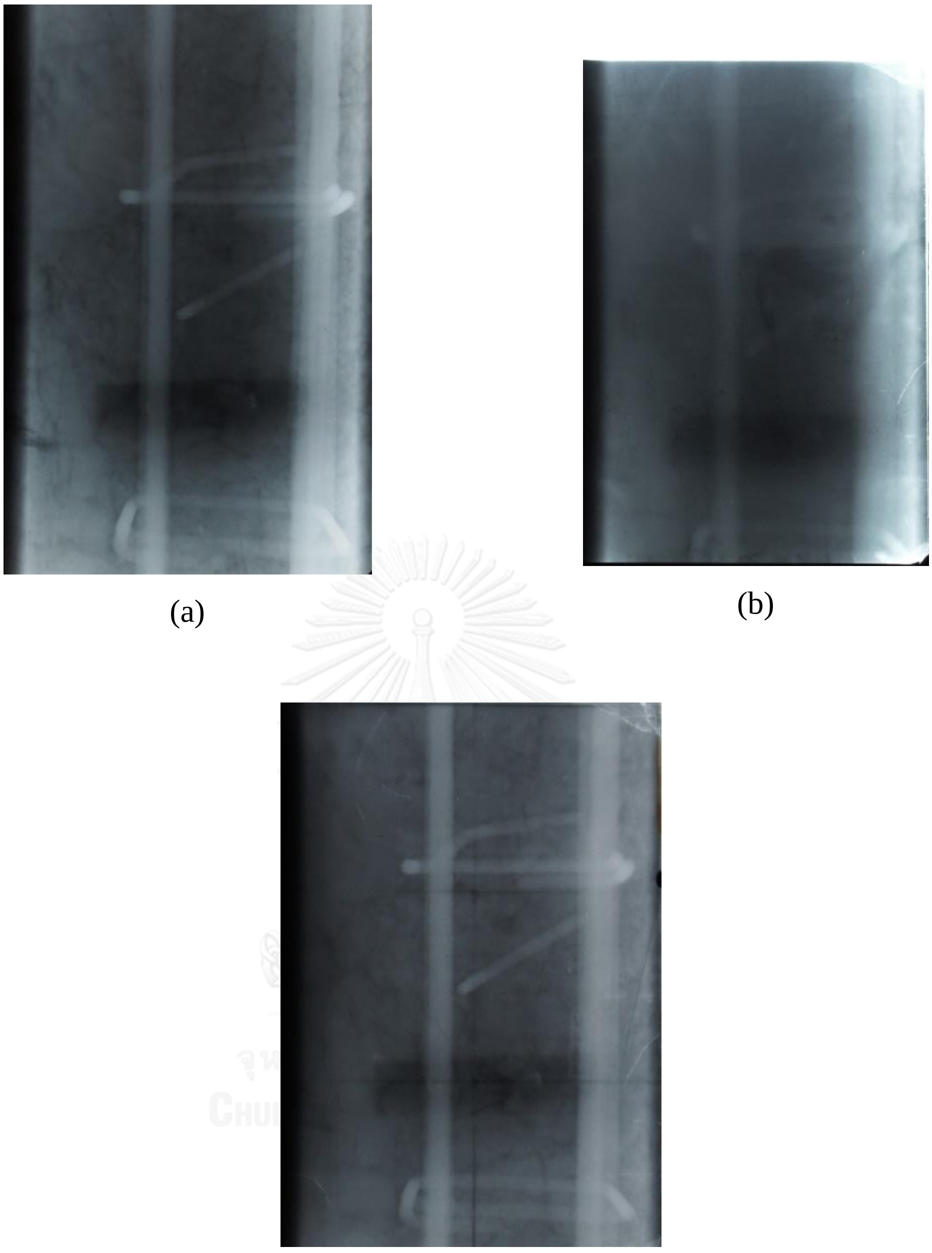

Figure 4.33 Radiographs of concrete pole taken with Ir-192 source

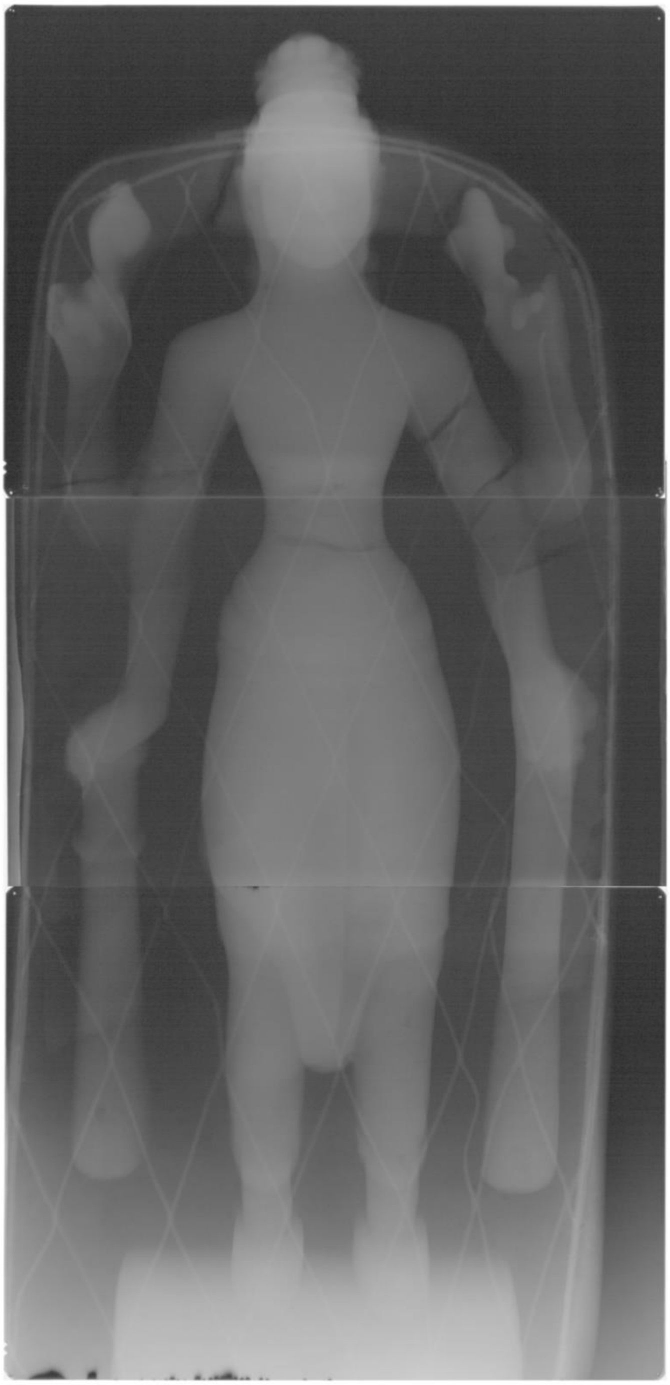

Figure 4.34 Radiograph of the Narayana statue using the lead screen-film technique taken with Ir-192 source

Figure 4.35 Radiograph of the Narayana statue using PI-200 screen-film technique taken with Ir-192 source

4.3 Determine the exposure time for gamma ray radiography by using the developed device

4.3.1 Radiation counting device using PIN photodiode

The transmitted gamma ray intensity was successfully measured by the developed device. The obtained transmitted gamma ray intensity versus steel thickness could be plotted as shown in figure 4.36.

From the results, the transmitted gamma ray intensity decreased with increasing steel thickness. The minimum count of all obtained counting data was found to be approximately 37,000 counts per 30 second. The standard deviation was therefore predicted from the square root of 37,000 which was approximately 192. The precision (3σ) was about 577 which was better than 2% at 99.7% confidence. The results showed that the uncertainty of gamma ray counting is lower than 2%. However, it can be decreased with increasing of the counting time.

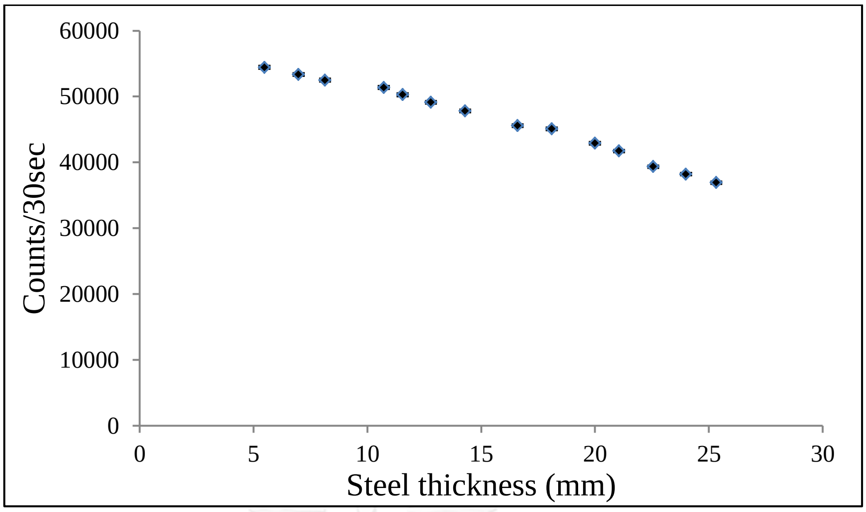

Figure 4.36 Relationship between the gamma ray intensity measured by the developed counting device and the steel thickness

4.3.2 Film optical density (OD) for various steel thicknesses

By varying the exposure times, the film OD increased with increasing the exposure time whereas it decreased with increasing the steel thickness. The obtained data were fitted with the linear function as shown in figure 4.37. To avoid overlapping of the fitted curves as shown in figure 4.37, only 10 out of 14 data sets from our experiments were selected to present.

The relationships of the transmitted gamma ray count rates and the calculated exposure times at various thicknesses were created by fitting the logarithmic function. Finally, the calibration chart from the developed method was achieved as shown in figure 4.39. The calibration chart obviously shows that the impact of counting uncertainty from the in-house developed device is small in determining the exposure time. The obtained calibration chart was then employed to determine the appropriate exposure time using the transmitted gamma ray intensity of and the test specimens, regardless of the thickness and kind of material.

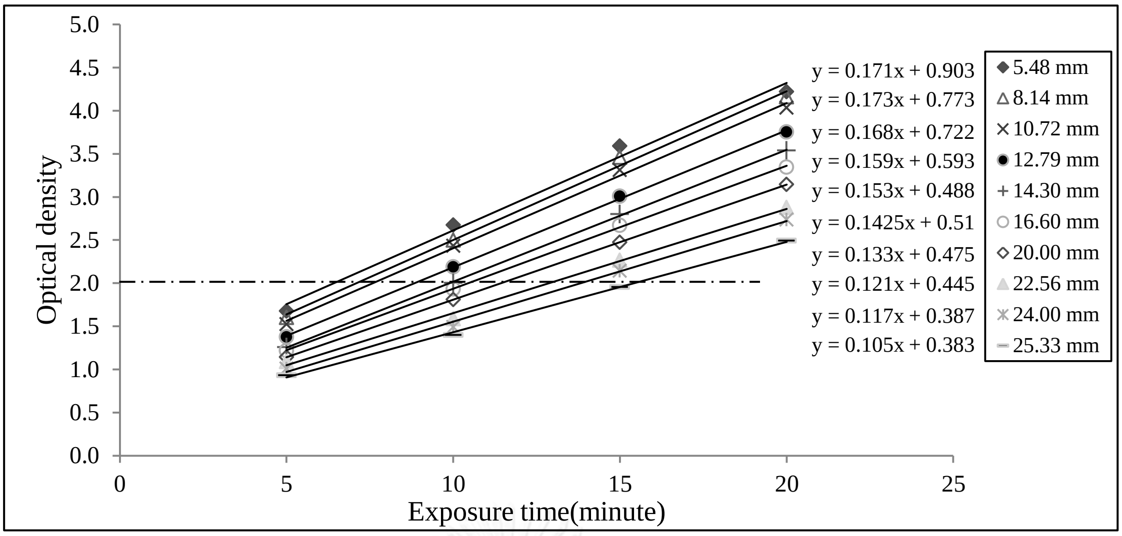

Figure 4.37 Relationships between the exposure times and the ODs at various thicknesses.

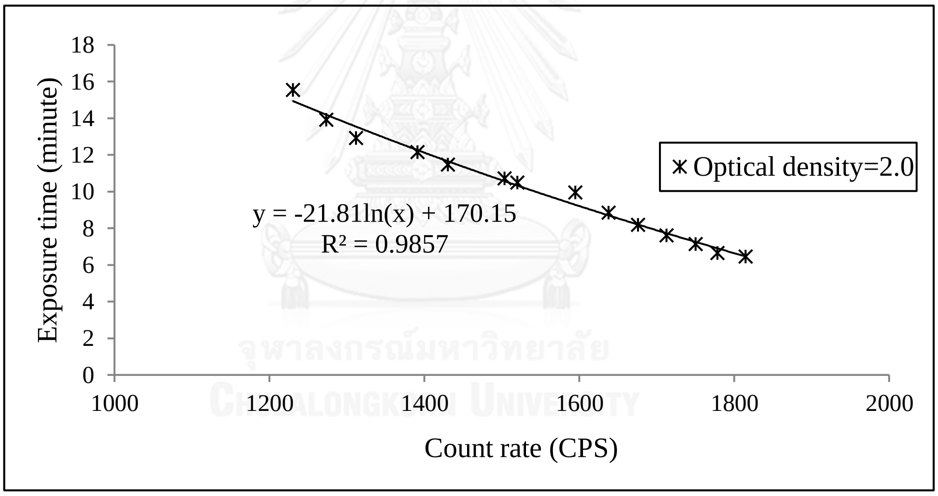

Figure 4.38 Calibration chart for the film OD at 2.0

4.3.3 Testing the developed device for determination of exposure time

By applying the developed method, the appropriate exposure time for the OD is 2.0 could be successfully determined using the measurement of the transmitted gamma ray intensity. The radiographic images were shown in figure 4.40. The film ODs were measured at the positions indicated by the squares in figure 4.40 where the PIN photodiode was placed to measure transmitted gamma ray intensity. The film ODs of a welded steel plate, a cast iron and a lock radiograph were found to be 2.05, 1.98 and 1.92, respectively, as shown in table 4.18. The discrepancies of the film OD were found to be very small compared to the expected film OD of 2.0. The obtained ODs were still in the acceptable range. Furthermore, the results indicated that the developed counting system and the calibration method could give appropriate exposure time without specimen information and any correction factor. However, film chemical quality of film processing should be strictly controlled.

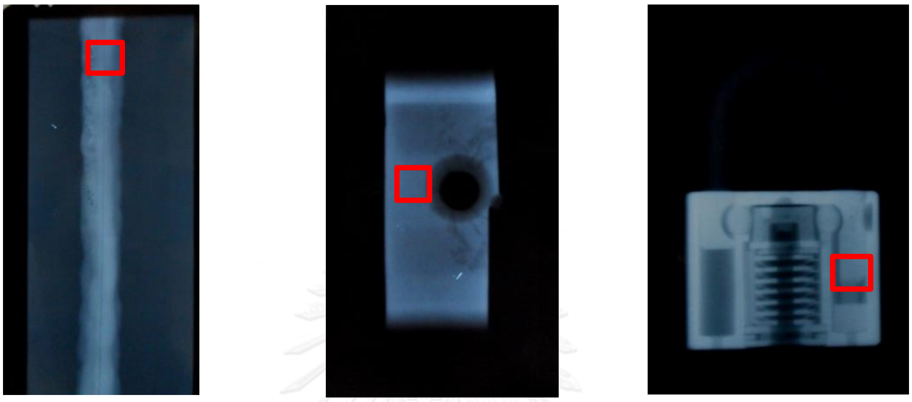

Steel welded seam　　Cast iron　　Lock

Figure 4.39 Radiographic of test specimens

Table 4.18 Film OD of the radiographic testing

Sample	Thickness (cm)	Gamma ray intensity (cps)	Exposure time (min)	(OD)	Discrepancy
Welded steel plate	0.8	1713	7.68	2.05	+ 0.05
cast iron	1.5	1530	10.14	1.98	- 0.02
Lock	2.0	1355	12.78	1.92	- 0.08

CHAPTER 5
CONCLUSION

Chapter 5 describes the conclusions and suggestion of this research.

5.1 Conclusion

5.1.1 Intensifying factor or speed exposure of screen-film

By studying the properties of various types of intensifying screen and energy radiation, we can conclude that type of screen and radiation energy affects directly to the speed of radiography. For the radiography using x-ray generator, PI-200 fluorescent screen is suitable for matching with model Kodak AA400 film type. It can increase exposure speed about 15 times compared with conventional film radiography, lead screen with Kodak AA400 film at 160 kVp voltage of x-ray. In case of radiography using gamma radiation source, PI-200 fluorescent screen shows the highest speed and higher than conventional lead screen- film radiography for Ir-192 radioisotope source at about 2.3 times.

5.1.2 Image quality of developed technique compared with conventional technique

By comparing of image quality from various screen-film types, the conventional lead-film technique provides the best image quality. However, PI-200-film provides the highest radiographic speed. To improve speed and image quality of radiographic technique, lead sheet filter coupled with PI-200 screen condition is properly applied to the radiographic technique.

5.1.3 Test specimens from developed radiographic technique compare with conventional film radiographic technique

By applying the developed technique to the real specimen in case of the Narayana statute, it can be seen that the speed of developed screen-film technique is faster than conventional screen-film method almost 3 times. However, image quality and detail of conventional screen-film is better than developed screen-film. Nevertheless, the developed screen-film radiographic technique is sufficient for providing the image quality and the detail of specimen for the view point of internal structure investigation. As same as the thick specimen like a concrete pole, the image quality using the developed technique can be improved by using lead filter.

5.1.4 Developed device for determination of the optimum exposure by measurement of the transmitted gamma ray intensity

Industrial radiography is actually not only used to radiograph industrial specimens. It is also widely used to inspect ancient objects and other large specimens like concrete structures and large animals. The latter is due to too low energy medical x-rays. Radiographers often have difficulty in determining appropriate exposures due to lack of appropriate calibration and specimen information The in-house developed gamma ray counting device combining with a smartphone and Bluetooth technology was successfully tested in this work. It can facilitates the experiment is more convenient and safer. Moreover, the developed device can be reduced of time to trial and error for radiographic technique at least equal time for setup geometry and film processing. The time for setup the radiographic technique geometry depend on skill and experience of radiographer the minimum about 5 minute and the part of film processing time minimum including the film drying about 30 minute from standard recommend manufacturer.

5.1.5 Determination of exposure using the developed technique and device with specimens

The calibration chart for the gamma ray radiography using film with Ir-192 source was successfully created by the development method. The new technique based on measurement of transmitted gamma ray intensity accompany with the calibration method could provide the appropriate exposure time with an expected optical density. Therefore, the method can help the radiographer to reduce time and cost loss from the trial and error of unknown specimen.

5.2 Suggestion

5.2.1 Other types of high speed film should be tested to further improve of the speed. For the PI-200 light emitting screen, photographic films may be more suitable and economical. There are actually more choices of photographic film and paper for future experiments.

5.2.2 Agfa RCF fluorometallic screen and Agfa NDT 1200 fluorescent screen claims their ultrahigh speed and good image quality. Future research on speed improvement should be experimentally tested for comparison.

5.2.3 The PIN photodiode detector showed its better sensitivity to x-ray and gamma ray at low dose rate but the CMOS showed its excellent sensitivity and linearity even at high dose rate range which is practical in industrial radiography. In addition, The CMOS image sensors of digital cameras and smartphones are also available at reasonable costs with functions readily for video recording which is needed for measurement of transmitted x-ray and gamma ray intensity. In this case the Wi-Fi camera will be available for measuring to determine the exposure time of film radiographic technique.

REFFERENCE

[1] U. Bulubay and A.Beril Tugrul, Quantitative evaluation of intensifying screen materials in Co-60 radiography for steel parts, NDT&E international, 31, 193-199, 1998

[2] R.C. Barrosoa, O.D. Gongalvesb, J. Eichler, R.T. Lopesds, S.C. Cardosoe, Study of secondary x-rays from radiographic intensifying screens, Nuclear Instruments and Methods in Physics Research A 404, 407-412, 1998

[3] I. Kandarakis, D. Cavourasa , G.S. Panayiotakisb, D. Triantisc, C.D. Nomicos, An experimental method for the determination of spatial-frequency-dependent detective quantum efficiency (DQE) of scintillators used in x-ray imaging detectors, Nuclear Instruments and Methods in Physics Research A 399, 335-342, 1997

[4] F. A. F. Zananiri and R. D. Speller**,** Dual energy radiography using X-ray films and intensifying screens, Journal Biomed. Eng. Vol.12 May 1990

[5] J.A de Raad, A. Kuiper, Industrial Radiography Image forming techniques, General electric company, inspection Technologies 2007

[6] T.S. Curry, J.E. Dowdey and R.C. Murry Jr. Christensen's Physics of Diagnostic Radiology 4 ed.Lea & Febiger, Pennsylvania, 1990.

[7] Introduction of Non-Destructive Testing Technique, Radiographic testing, The Hashemite University NDT center. [Online]. Available from: https://eis.hu.edu.jo/ACUploads/10526/ Radiographic%20Testing.pdf, [May 2015]

[8] Lecture Script for the IAEA/RCA Regional Training Course on Digital Industrial Radiology and Computed Tomography Applications in Industry, Kajang, Malaysia, 2 – 6 November 2009

[9] Radiography Testing Training Course Lecture Note, RIGAGU DENKI

[10] Staff of IAEA**.** Industrial radiography: Training course series No.3, Manual of the syllabi contained in IAEA-TECDOC-628**.** Austria: National Atomic Energy Agency, Vienna, 1992

[11] Richard A. Quinn Claire C. Editors, Radiography in Modern Industry, Eastman Kodak Company, NY, USA, 1980

[12] Carestream Health, Inc. Technical data/ Non Destructive Testing. INDUSTREX Film, NY, USA, 2014

[13] Staff of IAEA**.** Guide book of Non-Destructive Testing of concrete structure: Training course series No.17, IAEA-TCS-17. Austria: National Atomic Energy Agency, Vienna, 2002

[14] Feyzi Inanc, A monte carlo analysis of the lead screen impact on film radiography image formation, Quantitative Nondestructive Evaluation Vol.22, 2003

[15] Eastman Kodak Company. Technical Data/Non Destructive Testing Kodak Industrex AA400 Film, NY, USA, 2004

[16] Mitsubishi Chemical Coporation, [Online]. Available from: http://www.mcc-phosphor.com/english/products/x-ray/fluorescent/drz_pi.html 2009, Oct 2013

[17] MCI Optonix, LLC, AZ, USA 2015. [Online]. Available from: http://www.mcio.com/Products/intensifying-screen-rare-earth-blue.aspx, [May 2015]

[18] [Online]. Available from: http://www.kanchanaburi.go.th/au/tourkan_Eng/pongtuk.php, [Apr 2015]

[19] Han S K 2009 Fabrication and performance characteristics of a CsI(Tl)/PIN diode radiation sensor for industrial applications Appl. Radiat. Isotopes. 67 7

[20] Lucia A 2014 Comparison between a silicon PIN diode and a CsI(Tl) coupled to a silicon PIN diode for dosimetric purpose in radiology Nuclear Instruments and Methods in Physics Research A 762 11

[21] Ramírez-Jiménez F J 2003 Radiation detectors of PIN type for x-rays API 674 313

[22] Watanapanich P and Thong-Aram D 2014 Development of a smartphone based radiation survey meter The engineering institute of Thailand under H.M. The King's Patronage 25 105

[23] Hamamatsu Photonics K.K 2014 Silicon photodiodes (Solid State Division catalog February 2014)

[24] Hamamatsu Photonics K.K 1993 Silicon photodiodes and charge sensitive amplifiers for scintillation counting and high energy physics (Solid State Division catalog June 1993)

REFERENCES

APPENDIX

VITA

Mr. Chalermpong Polee was born on April 7, 1979 at Bangkok Thailand. He graduated from Department of Industrial Physics and Medical Instrumentation, Faculty of Applied Science, King Mongkut Institute of Technology North Bangkok in 2001 with a Bachelor of Science degree in Physics. In 2002, he started his word as a Scientist at Department of Nuclear Technology, Faculty of Engineering, Chulalongkorn University and he also studied in the same department and received Master of Science degree in Nuclear Technology in 2008. In 2008, he was awarded a fellowship by Ministry of Education, Science and Technology (MEXT), Government of Japan to research at Research Laboratory for Nuclear Reactors (RLNR), Tokyo Institute of Technology, Japan, for 1 year. In 2011 he joined for a doctoral degree in nuclear engineering at Department of Nuclear Engineering, Chulalongkorn University. He presented his research paper at the International Nuclear Science and Technology Conference (INST 2014) and published in Journal of Physics: conference series 611, 2015.